ASTRONOMY & ASTROPHYSICS
SUPPLEMENT SERIES

Astron. Astrophys. Suppl. Ser. **96,** 351-373 (1992)

Dynamic phenomena on the RS Canum Venaticorum binary II Pegasi in August 1989. I. Observational data

J.G. Doyle[1], B.J. Kellett[2], C.J. Butler[1], P.B. Byrne[1], J.E. Neff[3], A. Brown[4], D. Fox[4], J.E. Linsky[4], G.E. Bromage[2], S. Avgoloupis[5], L.N. Mavridis[6], J.H. Seiradakis[5], M. Mathioudakis[1], H.M. Murphy[1], J. Krzesinski[7], G. Pajdosz[7], V. Dadonas[8], J. Sperauskas[8], F. van Wyk[9], F. Marang[9], K. Olah[10], A. Collier Cameron[11], E. Antonopoulou[12], P. Rovithis[13] and H. Rovithis-Livaniou[12]

[1] Armagh Observatory, Armagh BT61 9DG, N. Ireland
[2] Astrophys. Div., Rutherford Appleton Lab., Chilton, Didcot, Oxon. OX11 0QX, U.K.
[3] Dept. of Astron. & Astrophys., The Pennsylvania State University, 525 Davey Lab., University Park, PA 16802, USA
[4] JILA, University of Colorado, Boulder, CO 80309, USA
[5] University of Thessaloniki, Dept. of Physics, Sect. of Astrophysics, Astronomy and Mechanics, GR-54006, Thessaloniki, Greece
[6] University of Thessaloniki, GR-54006, Thessaloniki, Greece
[7] Dept. of Astronomy, Pedagogical University, Krakow PL 30-084, Poland
[8] Vilnius Astronomical Observatory, Vilnius University, 232009 Vilnius, Ciurlionio, Lithuania
[9] South African Astronomical Observatory, PO Box 9, Observatory 7935, South Africa
[10] Konkoly Observatory, Hungarian Academy of Sciences, 1525 Budapest XII. Box 67, Hungary
[11] Astronomy Center, University of Sussex, Falmer, Brighton BN1 0QH, England
[12] Sect. of Astrophysics, Astronomy and Mechanics, Dept. of Physics, Univ. of Athens, Athens GR 15783, Greece
[13] Astronomical Institute, National Observatory of Athens, P.O. Box 20048, Athens 11810, Greece Physics, Univ. of Athens, Athens GR 15783, Greece

Received November 22, 1991; accepted March 23, 1992

Abstract. — Results are presented for two flares detected by the X-ray satellite GINGA, the International Ultraviolet Explorer satellite, ground-based Johnson *U*-band photometry, and optical spectroscopy from the Isaac Newton telescope for the RS CVn star II Peg. For the larger of these flares, we estimate the total optical energy in the 4000 – 6750 Å region to be at least 1.4×10^{36} erg. The contribution from emission lines in this spectral region is $\approx$ 3%. The X-ray flare spectra were fitted with single temperature Raymond-Smith type models which ranged from 65×10^6K towards the flare peak to 40×10^6K later in the decay phase, with the emission measure varying from 25×10^{53} to 13.6×10^{53}cm^{-3}. We estimate the total radiative energy in the 1 – 10 keV energy range to be $\sim 2 \times 10^{35}$ erg. The *U*-band flare energy is of the order of 4×10^{35} erg. During the flare, the hydrogen Balmer lines were substantially broadened, however, the Ca II K was only marginally broadened. Besides the normal strong lines such as Ca H & K, H δ and H γ, two other emission lines were present during the flare. The first of these was He I 4026Å, which has been observed previously during the impulsive phase of flares on dMe stars. However the second line has not been observed before, being due to Mn I 4032Å. For the quiescent X-ray spectrum a single temperature Raymond-Smith fit gives a rather poor fit. The best fitting results were obtained for a combination of a single temperature plasma together with a power-law to the data above 10 keV. The single temperature component implies a temperature of 12.4×10^6K with an emission measure of 1.5×10^{53}cm^{-3}. The iron abundance in the quiescent spectrum was close to solar, however for the flare spectra an abundance of 33% of solar was required to give acceptable fits.

Key words: RS CVn star – flare – X-ray spectra – Raymond-Smith models – Balmer emission lines – radio.

1. Introduction.

In a previous related paper (Doyle *et al.* 1991) we reported preliminary results of a large flare detected on the RS CVn type star II Peg in August 1989. The above paper reported only the GINGA X-ray and ground-based Johnson *U*-band observations. Here, we extend the earlier analysis by reporting on all the flare data obtained during that time; this includes ultraviolet spectra and optical photometry obtained with the International Ultraviolet

Explorer (IUE), optical spectra obtained with the Isaac Newton Telescope (INT) on La Palma, radio data obtained with the Very Large Array (VLA), plus additional photometric data from several other sites. In addition, we also present the quiescent data.

II Peg (=HD 224085) is a single-line spectroscopic binary of spectral type K2 IV-V with an orbital period of approximately 6.7 days. It is photometrically variable showing a wave-like variation, of the type usually interpreted as due to cool surface spots. Based on the photometric variability, II Peg was first classified as a BY Dra-type variable. A more detailed study by Rucinski (1977) however concluded that it was probably an RS CVn-type star. Rodonò *et al.* (1986,1987) and Byrne *et al.* (1987) reported on contemporaneous optical photometry and ultraviolet spectroscopy taken in 1981. The ultraviolet data indicated a modulation with phase in the sense that the maximum ultraviolet line emission was observed at phases near the minimum in the optical light curve, interpreted as due to the rotation of a solar-like active region. However, observations obtained since 1981 (e.g. Doyle *et al.* 1989a and Tagliaferri *et al.* 1991) now seem to indicate that these high points, observed most strongly in transition regions lines, such as C IV, could be flare related. In fact, there was a 7.5% probability that the 1981 high points were flare related (Doyle *et al.* 1989b), although at the time this was dismissed since the high points spanned almost two orbital rotations. In the 1986 data, Doyle *et al.* (1989a) reported evidence for a rotational modulation in lines such as Mg II h & k and O I 1305Å, which was quite different from the 1981 data reported by Rodonò *et al.* (1987) in the sense that the largest UV enhancement was observed when the major spot concentration was on the opposite hemisphere. Throughout the previous observing programmes connected with II Peg, several flares were observed in the UV region. However, none of these events was observed optically. The intention of this observing programme was to monitor II Peg in as many wavebands as possible for flare activity, the previous campaigns being orientated towards rotational modulation effects.

The paper is divided as follows. In Sect. 2 we outline the various datasets and their reduction. Section 3 is the results section, which includes details on the modelling of the X-ray data for both the large flare and the quiescent state. Finally, in Sect. 4 the various results are briefly summarised.

2. Observational data and reduction.

2.1. X-RAY DATA

The X-ray data were acquired by the Japanese X-ray satellite GINGA from 12:28 UT on 14 August to 03:33 UT on 17 August 1989. The instrument used was the Large Area Proportional Counter (LAC, see Turner *et al.* 1989 for further details), which is sensitive to photons in the energy range 1 to 35 keV. A description of the data and its reduction can be found in Doyle *et al.* (1991). The spectra were accumulated every 16 sec, with II Peg being detected in quiescence (non-flaring) throughout the observing period at approximately 6 cts s^{-1}. (It should be noted that due to the GINGA orbit for this target, the source was occulted by the Earth for $\sim$ 35% of the time. In addition the detectors were shut-off during passage through the South Atlantic Anomaly). During the period of monitoring, two X-ray flares were detected. The first of these on 16 August showed only a 30% enhancement over quiescence. The second, much larger flare was detected on 17 August, just after GINGA exited from the South Atlantic Anomaly. After an additional 35 min on-target, the satellite slewed to the next object. This second flare showed an X-ray enhancement of a factor of 30 over quiescence (see Fig. 1).

2.2. OPTICAL DATA

2.2.1. *Photometric data*

During a continuous 48 hr period of IUE observations beginning 22:40 UT August 14, 1989, a total of 32 photometric measurements were made using the Fine Error Sensor (FES). These FES counts were converted to give V magnitudes using a program given by Barylak (1989). According to the latter reference the uncertainty in V is ± 0.05 relative to the standard system but with internal errors much less.

Ground-based photometric observations were also obtained from several sources. Firstly, monitoring was carried out at Mt. Suhora Observatory (Poland), using a 60 cm Cassegrain telescope equipped with a double-channel photometer and blue and yellow filters which together approximate the Johnson B and V bands. The monitoring period was 15 August 20:28 to 16 August 01:59 UT, and 16 August 20:26 to 17 August 00:51 UT, with 30 sec integration times throughout. The local comparison star, BD +27°4648 was also measured which yielded a standard deviation in both filters of ± 0.006 mag. The second data set comprised $UBV(RI)_{KC}$ measurements made either once or twice per night for 29 nights over a four month period beginning mid-July 1989 at the South African Astronomical Observatory using the 50 cm telescope, equipped with a single channel photometer. The local comparison star in this case was BD +28°4667 (= HD 224084) with transformations to the standard system using E-region stars of Menzies *et al.* (1980). The third set of observations were performed with the 1m telescope on Mt. Maidanak in Uzbekistan, USSR using the standard set of glass filters of the Vilnius UPXYZVS system. The instrumental V values were transformed into the standard Vilnius system using linear relations derived from observations of Cygnus standard stars. The time resolution of the measurements

was of the order of 1 min, i.e. 10 measurements with an integration time of 1 sec in each filter. These observations were obtained 15:58 – 20:40 UT on August 15 and 15:31 – 19:00 UT on August 16. The local comparison star chosen was BD +28°4665 (= HD 224106). The observations on both the 15 and 16 August 1989 were obtained in five colors, $UBV(RI)_{KC}$, from Konkoly Observatory, Hungary. Again the comparison star chosen was BD +27°4648. Additional BV photoelectric observations were obtained on both of the above dates from the Kryonerion Astronomical Station using the 1.2m Cassegrain reflector of the National Observatory of Athens, Greece. Finally, a dataset was obtained from the Stephanion Observatory using the 0.75m Cassegrain reflector of the University of Thessaloniki. These observations were in UBV over the interval 3 to 14 August 1989. The comparison stars were BD +27°4648 and BD +28°4667 for the period 2 - 5 August, while for the remainder of the observations BD +27°4648 was replaced by BD +28°4665. A summary of the available photometric data can be found in the Appendix (Tables A1 to A6), while the magnitudes of the comparison stars are given in Table 1. In order to help identify the monitoring periods of the various telescopes/instruments we plot in Fig. 2 the time-lines for all the observations.

In addition to broad-band photoelectric measurements of the quiescent emission, flare monitoring data was also obtained at Stephanion during the GINGA, IUE and INT observations. This was in the Johnson U-band only, with the data being digitized every 6 sec. During the period from 22:10 UT on 14 August 1989 to 02:40 UT on 17 August, $\sim 13^h$ of monitoring was obtained, with three optical flares being detected (two of these being detected with GINGA and only one with IUE). Table 2 contains a summary of the monitoring intervals. On 17 August 1989, the largest of the three flares was detected; a light curve of this event, with both the U-band and X-ray data on the same time-scale, is shown in Fig. 1.

2.2.2. *Spectroscopic data*

Spectroscopic data in the blue (i.e. covering Ca II H & K to H γ) and the red (covering H α) were obtained on three nights; 14 August 22:38 UT to 15 August 05:17 UT, 15 August 22:59 UT to 16 August 06:09 UT and 16 August 22:26 UT to 17 August 06:03 UT on the Isaac Newton Telescope at La Palma. The telescope was equipped with the Intermediate Dispersion Spectrograph, a GEC blue-coated chip and a grating with a dispersion of 35 Å mm^{-1}. In the mode of observations, exposures of 60 sec in the blue and 30 sec in the red were made alternatively throughout the night. This gives an effective cycle time of approximately 4 mins. For the wavelength calibration, a CuAr arc was obtained every 2-3 hrs., and for calibration of the wavelength sensitivity, two or three standard stars were observed per night.

The data were reduced with the STARLINK packages: FIGARO (Fuller 1989) and DIPSO (Howarth & Murray 1987). The spectral resolution at Hδ was $\sim$ 1.4 Å and at Hα it was $\sim$ 1 Å. The instrumental response and wavelength sensitivity were removed by comparing with spectra of standard stars taken with the same grating and slit setting. Absolute flux calibration was also through comparison with these standard stars. The accuracy of our flux calibration was checked by comparing the blue and red continuum flux with the broad band B and R fluxes using the calibration of Bessell (1979). The agreement was within 20% to 30%.

2.3. ULTRAVIOLET DATA

Ultraviolet spectroscopic data were obtained continuously over approximately a two day period beginning at 22:40 UT on 14 August 1989 to 21:00 UT on 16 August, with the International Ultraviolet Explorer (IUE) satellite. We obtained a 30 min. high dispersion LWP (1900 - 3200 Å) exposure ($\sim$ 0.2 Å spectral resolution) followed by a double low dispersion SWP (1150 - 1950 Å) exposure ($\sim$ 5 Å spectral resolution) on the same image, each of these exposures being 30 min. A log of the observations is given in Table 3. The spectra were extracted from the IUE images using the STARLINK package IUEDR (Giddings 1983). Once extracted, these spectra were then further analysed using DIPSO.

2.4. RADIO OBSERVATIONS

II Peg was observed using the NRAO[1] Very Large Array on 1989 August 15 over the period 08:45 - 14:55 UT and on August 16 over the period 08:42 - 15:19 UT. The array was split into two subarrays; one observing continuously at 6 cm, while the other observed alternatively at 3.6 cm and 20 cm. At each frequency two adjacent 50 MHz bandpasses were used. The observing frequencies were 8.465 and 8.415 GHz (3.6 cm), 4.885 and 4.835 GHz (6 cm), and 1.515 and 1.465 GHz (20 cm). A nearby phase calibrator was observed at roughly 25 minute intervals, 3C48 being used as the primary flux calibrator with assumed flux densities of 3.29, 5.60, and 15.47 Jy at 3.6, 6 and 20 cm respectively. Data from the two bandpasses in each band were combined to increase the stellar signal. The data were calibrated and reduced using standard Astronomical Image Processing System (AIPS) routines. Radio light curves were derived using the AIPS routine DFTPL.

[1] The National Radio Astronomy Observatory is operated by Associated Universities, Inc., under National Science Foundation Cooperative Agreement AST-8814515.

3. Results

3.1. QUIESCENT STATE

3.1.1. *Photometric data*

In Fig. 3 we show the V-band data for II Peg as a function of phase, using the orbital ephemeris of Vogt (1981), i.e.

$$JD_o = 2443033.47, \quad P_{\rm orbital} = 6.72422 \text{ days}$$

The overall agreement between the various datasets is very good, with zero point shifts of the order of 0.02 mag being required to bring the various light curves into agreement. The magnitudes for the three comparison stars can be found in Table 1. The large cyclic variations of $\Delta V = 0.45$ is similar to the 1986 value of 0.5, implying perhaps 40% of one hemisphere covered by spots (Doyle *et al.* 1988). In addition to the over-all photometric variability mentioned above, the FES data shows a symmetric 0.15 mag. "dip" just after phase 0.0, lasting a total of ~ 8 hrs. This type of short-term variation has not been observed previously. We have been unable to find any instrumental reason, although further observations are required. There are three possible explanations which include:

3.2. A PROMINENCE

The "dip" could be the result of an eclipse due to a cloud of neutral hydrogen high in the corona. Such cool clouds of gas have been observed on rapidly rotating K & M dwarfs, e.g. Collier Cameron & Robinson (1989) and Doyle & Collier Cameron (1990). An indication of cool dense material being present high in the atmosphere of II Peg during a flare has been reported previously by Doyle *et al.* (1989). However, a major problem with this interpretation is that although prominences have been observed in absorption lines such as H α, Ca II H & K etc., no such feature has been dense enough to be optically thick in the visible continuum.

3.3. A COMPANION

The secondary in the II Peg system has yet to be observed, but one possible interpretation of the photometric "dip" is that it is due to an eclipse by the companion since phase 0.0 is defined as the time when the primary is furthest from the observer. Taking the effective temperature of the primary to be $\sim$ 4700 K and a radius of $2.8R_\odot$, and assuming the eclipse is total and ignoring limb-darkening, we find the radius of the secondary to be $\sim 1R_\odot$. This value is not critically dependent upon the surface brightness of the secondary. The phase difference between the first and fourth contact is $\sim 20^o$, hence the orbital separation between the components would be $(R_1 + R_2)/sin\,10$, i.e. $\sim 20R_\odot$. Furthermore, we find the mass of the secondary to be $\sim 0.6M_\odot$, the primary $\sim 2M_\odot$ and a luminosity ratio between the components of ~ 0.05. The above estimated radius and mass of the secondary would imply an M dwarf of spectral type M0.

3.4. A FLARE

An alternative explanation is that the increase in the FES mag. beginning at phase 0.95 is due to a large flare, with the flare decay beginning at phase 0.01 and ending at phase 0.04. In this interpretation, the rising part of the apparent "dip" is simply the under-lying spot light-curve. Using the V-band flux calibration of Bessell (1979), implies a V-band flare energy of $\sim 1.2 \times 10^{36}$ erg. Other large energetic flares have being observed on II Peg previously, e.g. Doyle *et al.* (1989) estimated a total radiative energy of 2.4×10^{36} erg for a flare observed with IUE. However, if this is a flare, there is no corresponding increase in the simultaneous IUE data which one would expect for such an energetic event.

3.4.1. *X-ray data*

In Table 4 we present the results of the spectral fits to the quiescent X-ray spectrum, which was summed over the entire period of GINGA observations, excluding the periods of flare activity. The fitting procedure was performed for combinations of Raymond & Smith model plasmas and power-law photon distributions. Since II Peg is at 30 pc, the line-of-sight absorbing column density is essentially zero. The best fitting results were obtained for a combination of a single temperature plasma together with a power-law. The quiescent spectrum is incompatible with a single temperature model alone. Two-temperature models do result in a very high, but uncertain, temperature ($T_e > 10^8$ K) for the second component. The reason for this second high temperature component is the tail in the photon distribution, which extends up to 18 keV (see Fig. 4). We have made extensive efforts to check the validity of this high energy emission. We do not believe it is due to background subtraction problems: II Peg lies well away from the galactic plane ($l = 108.2°, b = -32.6°$), and it would require an excess of $\sim$ 10% over the 'average' diffuse hard X-ray background. This is equal to the galactic contribution *towards* the galactic centre (Iwan *et al.* 1982). In fact II Peg is situated in a region of the galaxy where the hard X-ray background is within 1.5% of the mean intensity (Iwan *et al.* 1982). We can also rule out a second source in the field, since neither the EINSTEIN Observatory nor EXOSAT reported any other point sources in the field of II Peg. Therefore we decided to add a power-law component. This resulted in a considerable improvement of the reduced chi-square. Of the fits which consist of a one-temperature plasma and a power-law, the one with a slight over-abundance of iron gives the lowest value of the reduced chi-square.

The 'best-fit' results that we will use is a temperature of $T_e = 12.4 \times 10^6$ K and emission measure

$EM = 1.5 \times 10^{53}\mathrm{cm}^{-3}$. The results for the power-law component $\{J(\epsilon) = A\epsilon^{-\gamma}\,\mathrm{ph\,cm^{-2}\,s^{-1}\,keV^{-1}}\}$ are $A = 1.86 \times 10^{-3}$ and $\gamma = 2.05$. It is necessary that the power-law distribution turns over and becomes steeper somewhere above 18 keV (this being the high energy cut-off of the present observations), otherwise the total flux $\{\int_0^\infty J(\epsilon)\epsilon d\epsilon\}$ becomes infinite. The total radiative losses by the power-law component between 1 and 18 keV is $9 \times 10^{29}\mathrm{erg\,s^{-1}}$.

3.4.2. *Ultraviolet data*

Line fluxes of the prominent emission lines were derived by least-squares Gaussian fits. These are given in Tables 5 and 6. The *FWHM* of the fitted lines were consistent with the instrumental width of $\sim$ 5Å for low resolution SWP spectra (Cassatella *et al.* 1985). The derived line fluxes at Earth were reduced to surface fluxes at the star using the conversion factor from Table 7 of Rodonò *et al.* (1986), i.e. 2.3×10^{17} . In Fig. 5a, we show the C IV 1550Å flux as a function of time from 14 August 23:00 UT to 16 August 21:00 UT. With the exception of one (and perhaps two) flare(s) on August 16, there is no evidence for a modulation. However, the Mg II h & k plotted over the same time interval (Fig. 5b) show's evidence for a steady increase in flux. This is in phase with the *V*-band light-curve (i.e. increasing plage activity with decreasing number of spots) and is similar to that noted by Doyle *et al.* (1989a) for 1986 II Peg data but is opposite to the 1981 data reduced by Rodonò *et al.* (1987).

In this spectral region there are three possible line ratios which we can be used to determine the electron density in the transition region, viz C III 1176/C III 1908, Si III 1892/C III 1908 and Si IV 1396 & 1403/C III 1908. However, in the mean quiescent spectra we are unable to derive a reliable line flux for either the C III 1908Å or the Si III 1892Å lines, although an upper limit of $4 \times 10^{-14}\,\mathrm{erg\,cm^{-2}\,s^{-1}}$ is indicated. In fact, Doyle *et al.* (1989b) give fluxes of $5 \times 10^{-14}\,\mathrm{erg\,cm^{-2}\,s^{-1}}$ for these lines (based on 1983 data), indicating an electron pressure of $P_e/k = 6 \times 10^{14}\,\mathrm{cm^{-3}\,K}$.

3.4.3. *Radio data*

The 6 cm quiescent flux on August 15 showed a 'steady' increase from 1 mJy to 2.75 mJy some 6 hrs later, with a mean value of 1.922 ± 0.040 mJy (see Fig. 6). Unfortunately, the 3.6 cm data has calibration problems while the 20 cm data is severely compromised by the presence of a very strong confusing source, hence mean fluxes for these bands for August 15 was not possible. For the second day's data, mean fluxes of 1.94 ± 0.05, 2.34 ± 0.08, & 1.50 ± 0.27 mJy at 3.6, 6 and 20 cm were derived. On August 16, the 6 cm data showed the opposite effect of the previous day's data, decreasing from a mean value of 3.5 mJy to 2.0 mJy while the 3.6 cm data decreased from 2.5 to 1.4 mJy over the 6 hr. period of our observations. It is interesting to note that the increase in the 6 cm flux on August 15 corresponds to a steady increase in the GINGA X-ray quiescent flux, while for August 16, the 6 cm flux decreased as the X-ray flux decreased.

3.5. Flare State

3.5.1. *Photometric data*

Prior to these observations of II Peg, broad-band optical flare activity on RS CVn stars has only been reported once, i.e. Patkos (1981). The absence of such optical flares was generally interpreted as due to a contrast effect since the brightness of the stellar photospheric continuum in these stars is several orders of magnitude more than the dMe stars. However the observations obtained from the Stephanion Observatory would tend to dispel that idea. Similar to the analysis of *U*-band data from dMe stars, the flare's equivalent duration in units of time is given by

$$E = \sum_f [(I_f - I_0)/I_0]\Delta t$$

where I_0 is the intensity deflection due to the star in its quiescent state after sky subtraction and I_f the intensity due to the star in its flare state less sky background and Δt is the *U*-band integration time. A summary of the derived *U*-band parameters for each of the three flares is given in Table 7.

Unfortunately, due to sunrise, the optical observations for the large flare of 17 August ceased before the flare ended, therefore only 48 min. of *U*-band data were acquired. The equivalent duration was multiplied by the star's quiescent luminosity, implying a flare energy of at least 1.8×10^{35} erg. (Note that we took the quiescent *U*-band luminosity as that prior to the flare and multiplied by the flux calibration of Bessell 1979). The above value is obviously a lower limit since we do not know how long the optical flare lasted. However, from the estimated duration of the flare as observed by the INT, we could have under-estimated the *U*-band flare energy by more than a factor of two, implying a total *U*-band energy of perhaps $\sim 4 \times 10^{35}$ erg, (see Doyle *et al.* 1991 for further details). The second of the flares on 16 August at 01:15 UT (i.e. the one where we have simultaneous optical spectra, X-ray and UV data) had a *U*-band energy of 9×10^{32} erg. Although photometric monitoring was also continuing from Mt. Suhora Observatory during the time of these flares on August 16, this latter dataset was in *V* and *B* and the flares were not intense enough to register a signal. The *U*-band flare at 00:51 UT on 16 August had a *U*-band energy of 4×10^{32} erg.

3.5.2. *Optical spectra*

During the period of spectroscopic monitoring, two flares were detected. The first on 16 August at ~ 01:15 UT and the second on 17 August beginning at approximately 02:00 UT. Below, we discuss each of these events in more detail.

We consider first the flare of August 17. In the blue, the flare continuum show a 80% enhancement over pre-flare, while in the red, the enhancement was approximately 10%. The flare rise-time was very gradual, taking approximately 30 min. to reach maximum. The flare-only spectrum in the blue (i.e. a mean quiescent spectrum has been subtracted) is shown in Fig. 7 at two times during the flare; the first being at flare maximum (~ 02:18 UT) while the second was late in the decay phase (~ 04:50 UT). Besides the normal strong lines such as Ca II H & K, Hδ and Hγ, two other emission lines are present. The first of these is He I 4026Å, which has been observed previously during the impulsive phase of flares on dMe stars. However the second line has not been observed before. We conclude that it is due to Mn I 4032Å, normally considered a photospheric line. In fact, in the quiescent spectrum, there are three Mn I lines which form a deep absorption feature at 4032Å. The resultant feature is shown in Fig. 8, where we have taken a flare spectrum towards the end of the flare (given by the solid line) and superimposed the mean quiescent spectrum (a small flux of 0.1×10^{-12} erg cm^{-2} s^{-1} has being added to the quiescent spectrum in order to match the depth of other absorption features close to Mn I). Note that in the Mn I feature there is a small self-reversal. This is the emission feature that we observe throughout the flare.

In Fig. 9a, we plot the flare flux in two of the strong emission lines, Ca II K 3933Å and Hδ as a function of time. The duration of the flare was at least 4 hr., with a secondary event occurring at 5:15 UT. In Fig. 9b we show the variation of the *FWHM* of the above lines, obtained by means of Gaussian fits to the lines. The width of the Ca II K line at the beginning and at the end of the flare is consistent with the instrumental width, however Hδ is substantially broader. Note that both the *FWHM* and line flux of the Ca II K peaks some 20 min. later than H δ. The line fluxes during the 17 August flare in Hα, Hγ, Hδ and Ca II K is given in Tables 8 and 9. Note that in the quiescent state, Balmer lines such as Hγ and Hδ are very weak.

The total continuum energy for this flare was derived by taking flux measurements near 4000 Å, 4250 Å, 6400 Å and 6750 Å and assuming that the continuum varied linearly between these points, the flux from 4000 Å to 6750 Å (in erg cm^{-2} s^{-1}) was derived for each spectrum. Using this procedure on all the spectra, we thus generated a series of flux measurements (i.e. integrated over wavelength) throughout the duration of the flare, as plotted in Fig. 10. Integrating these fluxes over the duration of the observations, we obtained a total energy of $> 1.4 \times 10^{36}$ erg in the spectral region from 4000 Å to 6750 Å, where we have used the distance ($d = 29.4$ pc) to II Peg. The total energy in the emission lines, i.e. Hα, Hβ, Hγ, Hδ, Hϵ, Ca II H & K (under the assumption that H$\beta \sim H\gamma$ and Ca II H ~ Ca II K), relative to the continuum, for the same time interval is 3.9×10^{34} erg. This is approximately 3% of the total radiative losses in the optical region.

The flare of 16 August started at ~ 01:15 UT and had a duration of less than 30 min. The maximum enhancement factor over quiescent was less than 50% in the blue and ~ 6% in the red. Using the same procedure as before, we estimate the total flare energy in the 4000 to 6750Å region to be ~ 2.5×10^{34} erg.

3.5.3. *UV* DATA

Unfortunately, the monitoring by the IUE satellite ceased a few hours before the large flare of 17 August 1989. However, at least one and perhaps two smaller flares were observed on 16 August 1989 with IUE, these being at 01:15 UT and 12:16 UT. Below we discuss the first of these flares. However, in order to discuss the properties of this flare, we must first isolate the radiation of the flare from the background quiescent stellar flux by subtracting the mean quiescent spectrum from each of the flare spectra. Henceforth when we speak of the "flare" it will be implicit, unless stated otherwise, that it is these background corrected spectra and their fluxes that we are referring to.

During the flare exposure, the Si III 1892Å line is enhanced over the quiescent. However, a determination of the C III 1908Å line is still not possible. Hence we are unable to estimate the electron density in the transition region of this flare as we have done in previous work (Doyle *et al.* 1989b).

3.5.4. *X-ray data*

The LAC spectra for the flare of 17 August were fitted with single temperature Raymond-Smith type-models (Raymond & Smith 1977) with temperatures which ranged from 5.5 keV to about 3.5 keV late in the flare decay. A proper fit to the Fe XXV line implied an iron abundance of 33% of that used by Raymond & Smith (1977), i.e. log [Fe] = 7.10. With the exception of the iron abundance, all other parameters were fixed at default solar values. The column density was fixed at zero, as mentioned in the quiescent state analysis. Examples of the quality of the spectral fits for the large flare can be found in Doyle *et al.* (1991). The flare temperature declined from at least 65×10^6 K to 40×10^6 K, while the EM decreased from at least 25×10^{53} to 13.6×10^{53} cm^{-3} during the period of X-ray observations (see Table 10 for further details). Integrating over the X-ray flux energy points implies a total X-ray flare energy of at least 4.6×10^{34} erg. This however is a lower limit to the total

flare energy as we observed neither the beginning nor end of the flare.

The method used by Doyle *et al.* (1991) for estimating the total X-ray energy is the "smooth burst model", where the integrated flux $f(t)$ is given by

$$f(t) = A B^{\beta} e^{-\frac{(t-t_{\rm start})}{t_{\rm d}}}$$

where $B = \frac{(t - t_{\rm start})\, e^1}{\beta\, t_{\rm d}}$, $t_{\rm d}$ is an exponential decay time (in hrs.), $t_{\rm start}$ the start time of the flare (assumed to be 02:03 UT as given by the optical data), and A the peak value of the flare. The total X-ray energy is then given by

$$L_x = 4\pi d_{\rm pc}^2\, 3.6 \times 10^{38} \int f(t){\rm d}t \quad {\rm erg}$$

where $d_{\rm pc}$ is the source distance in parsecs. A range of β values from 0.1 to 5 were tried. Example fits for four of these values are given in Fig. 11, and Table 11 gives the range of total integrated energies possible for $\beta = 0.1 - 5$. However, if we use the optical data to constrain the X-ray flare to peak at $\sim$ 02:30 UT, this requires $\beta \sim 1$ and $t_{\rm d} = 0.36$. This gives a total emitted X-ray energy of 1.84×10^{35} erg. From Table 11 this value is good to better than a factor of two.

For the flare of August 16, there is only sufficient data for one spectrum, giving average energy losses of $\sim 9 \times 10^{29}$ erg s^{-1}. Integrating over the time interval of the flare implies a total energy of $\sim 8 \times 10^{32}$ erg.

4. Summary

For the quiescent X-ray spectrum a single temperature Raymond-Smith fit give a rather poor fit. The best fitting results were obtained for a combination of a single temperature plasma together with a power-law. For a two-temperature model, the temperature of the second component was very high ($T_e > 10^8$ K). The reason for this second high temperature component is the tail in the photon distribution, which extended up to 18 keV. Extensive efforts were made to check the validity of this high energy emission. We do not believe it is due to background subtraction problems as it would require an excess of $\sim$ 10% over the 'average' diffuse hard X-ray background. We also rule out a second source in the field, since neither the EINSTEIN Observatory nor EXOSAT reported any other point sources in the field of II Peg. The single temperature component implies a temperature of 12.4×10^6 K with an emission measure of 1.5×10^{53}cm^{-3}.

The photometric flare data implies a U-band energy for the 17 August flare of at least 4×10^{35} erg. The small flare on 16 August had a U-band energy almost three orders of a magnitude smaller. Spectroscopic data for the larger flare implies an energy output between 4000 and 6750Å of at least 1.4×10^{36} erg, making this one of the largest optical flares ever observed. The X-ray flare spectra could all be fitted with a single temperature Raymond-Smith models which ranged in temperature from 65×10^6 K towards the flare peak to 40×10^6 K later in the decay phase, with the emission measure varying from 25×10^{53} to 13.6×10^{53}cm^{-3}. The total emitted X-ray energy was of the order of 1.8×10^{35} erg. During the flare the iron abundance was reduced by a factor of three.

In the follow-up paper, Doyle *et al.* (1992) will discuss in more detail the implications and interpretation of this rather vast data-set.

Acknowledgements.

We would like to thank the GINGA and IUE Observatory staff for their help in obtaining this data. Research at Armagh Observatory is grant-aided by the Dept. of Education for N. Ireland. We also acknowledge the support provided in terms of both software and hardware by the STARLINK Project which is funded by the UK SERC. Research at the Stephanion Observatory is grant-aided by the Empirikos Foundation. One of us (MM) would like to thank C. Papantoniou for valuable assistance during his observing run at Stephanion and Armagh Observatory for a research studentship. We also wish to thank Dr. M. Barylak for discussions concerning the FES onboard IUE and to Dr. G.H.J. van den Oord for many helpful comments on an earlier draft.

References

Barylak, M., 1989, ESA IUE Newsletter 33,20

Bessell, M.S., 1979, PASP 91,589

Byrne, P.B., Doyle, J.G., Brown, A., Linsky, J.L., Rodonò, M., 1987, A&A 180,172

Cassatella, A., Barbero, J., Benvenuti, P., 1985, A&A 144,335

Doyle, J.G., Butler, C.J., Morrison, L.V., Gibbs, P., 1988, A&A 192,275

Doyle, J.G., Butler, C.J., Byrne, P.B., Rodonò, M., Swank, J., Fowles, W. 1989a, A&A 223,219

Doyle, J.G., Byrne, P.B., van den Oord, G.H.J., 1989b, A&A 224,153

Doyle, J.G., Kellett, B.J., Byrne, P.B., Avgoloupis, S., Mavridis, L.N., Seiradakis, J.H., Bromage, G.E., Tsuru, T., Makishima, K., McHardy, I.M., 1991, MNRAS 248,503

Doyle, J.G., van den Oord, G.H.J., Kellett, B.J., 1992, A&A (in press - Paper II)

Fuller, N.M.J., 1989, 'FIGARO' Starlink User Note 86, Rutherford Appleton Lab.

Giddings, J.R., 1983, 'IUEDR' Starlink User Note 37, Rutherford Appleton Lab.

Howarth, I.D., Murray, M.J.,, 1987, 'DIPSO' Starlink User Note 50, Rutherford Appleton Lab.
Iwan, D., Marshall, F.E., Boldt, R., Mushotzky, R.F., Shafer, R.A., Stottlemyer, A., 1982, ApJ 260,111
Menzies, J.W., Banfield, R.M., Laing, J.D., 1980, SAAO Circ. 1,149
Patkos, L., 1981, Ap L 22,1
Raymond, J.C., Smith, B.W., 1977, ApJS 35,419
Rodonò, M., Cutispoto, G., Pazzani, V., Catalano, S., Byrne, P.B., Doyle, J.G., Butler, C.J., Andrews, A.D., Blanco, C., Marilli, E., Linsky, J.L. Scaltriti, F., Busso, M., Cellino, A., Hopkins, J.L., Okazaki, A., Hayashi, S.S. Zeilik, M., Helston, R., Henson, G., Smith, P., Simon, T., 1986, A&A 165,135
Rodonò, M., Byrne, P.B., Neff, J.E., Linsky, J.L., Simon, T., Butler, C.J.,Catalano, S., Cutispoto, G., Doyle, J.G., Andrews, A.D., Gibson, D.M., 1987, A&A 176,267
Rucinski, S.M., 1977, PASP 89,280
Tagliaferri, G., White, N.E., Doyle, J.G., Culhane, L.J., Hassall, B.J.M., Swank, J.H., 1991, A&A 251,161
Turner, M.J.L., Thomas, H.D., Patchett, B.E., Reading, D.H., Makishima, K., Ohashi, T., Dotani, T., Hayashida, K., Inoue, H., Kondo, H., Koyama, K., Mitsuda, M., Ogawara, Y., Takano, S., Awaki, H., Tawara, Y., Nakamura, N., 1989, PASJ 41,345
Vogt, S.S., 1981, ApJ 247,975

TABLE 1. *Magnitudes for the three comparison stars used to calibrate the photometric data for II Peg.*

Star	Sp. ty.	V	(U-B)	(B-V)	(V-R)	(V-I)
HD224084	K0	8.24	1.36	1.29	0.64	1.25
BD+27 4648	G5	9.41	0.84	1.04	0.78	1.31
HD224016	G5	8.54	0.49	0.79	0.61	1.01

TABLE 2. *A summary of the U-band monitoring intervals for II Peg during the period 14-17 August 1989 obtained from Stephanion.*

Date	Monitoring intervals (UT)	Total monitoring time
14/15 Aug	22:10 - 22:49, 22:51 - 23:42, 23:44 - 23:47	
	00:08 - 01:02, 01:06 - 02:14, 02:16 - 02:29	03:48
15/16 Aug	20:52 - 21:23, 21:27 - 21:58, 22:09 - 22:55	
	22:58 - 23:46, 23:50 - 00:34, 00:49 - 01:36	
	01:39 - 02:30	04:58
16/17 Aug	20:50 - 21:58, 22:13 - 23:05, 23:08 - 23:30	
	23:36 - 00:03, 00:07 - 00:14, 00:24 - 01:04	
	01:23 - 01:48, 01:52 - 02:40	04:49

TABLE 3. *A log of the IUE observations obtained for II Peg in August 1989. Some of the images were double exposures, these are labelled A and B.*

Date	UT (start)	Image	Exp.(min)	Date	UT (start)	Image	Exp.(min)
14 Aug	22 42 05	LWP16125	30	15 Aug	21 42 14	SWP36853B	30
	23 40 26	SWP36844A	25		22 39 54	LWP16134	30
15 Aug	00 24 45	SWP36844B	25		23 24 56	SWP36854A	30
	01 00 11	LWP16126	30	16 Aug	00 03 59	SWP36854B	30
	01 41 09	SWP36845A	30		00 44 30	LWP16135	30
	02 17 34	SWP36845B	50		01 25 06	SWP36855A	30
	06 32 56	SWP36846A	30		02 06 33	SWP36855B	30
	07 12 18	SWP36846B	30		02 41 33	LWP16136	27
	07 52 04	LWP16127	30		06 36 04	SWP36856A	30
	08 33 48	SWP36847A	30		07 21 47	SWP36856B	30
	09 12 47	SWP36847B	30		08 02 17	LWP16138	30
	09 53 00	LWP16128	30		08 46 10	SWP36857	30
	10 36 04	SWP36848A	30		09 26 17	LWP16139	30
	11 15 01	SWP36848B	30		10 07 22	SWP36858A	30
	11 55 10	LWP16129	30		10 46 22	SWP36858B	30
	12 35 36	SWP36849A	30		11 28 13	LWP16140	30
	13 17 30	SWP36849B	30		12 16 41	SWP36859	45
	13 57 36	LWP16130	30		13 11 46	LWP16141	30
	14 56 05	SWP36850A	30		13 49 00	SWP36860	45
	15 40 56	SWP36850B	30		15 18 40	LWP16142	30
	16 21 57	LWP16131	30		15 57 40	SWP36861	30
	17 06 16	SWP36851A	30		16 41 08	LWP16143	30
	17 41 25	SWP36851B	30		17 43 28	SWP36862A	30
	18 22 45	LWP16132	30		18 22 53	SWP36862B	30
	19 05 26	SWP36852A	30		19 00 20	LWP16144	30
	19 42 01	SWP36852B	30		19 43 46	SWP36863A	30
	20 20 42	LWP16133	30		20 21 59	SWP36863B	30
	21 05 55	SWP36853A	30		21 01 07	LWP16145	35

TABLE 4. *Best fit spectral parameters* (II Peg in quiescence).*

PARAMETER	SPECTRAL MODELS					
	RS	RS	RS+PL	RS+PL	RS+RS	RS+RS
RS EM_1	$1.80^{+0.06}_{-0.05}$	$1.65^{+0.08}_{-0.07}$	$1.68^{+0.21}_{-0.40}$	$1.52^{+0.31}_{-0.59}$	$1.74^{+0.12}_{-0.11}$	$1.77^{+0.09}_{-0.07}$
RS kT_1	1.74 ± 0.07	1.77 ± 0.06	$1.12^{+0.18}_{-0.26}$	$1.07^{+0.24}_{-0.29}$	1.20 ± 0.10	$1.18 \pm .07$
RS Fe	1.00	2.27 ± 0.48	1.00	$1.69^{+2.62}_{-0.92}$	1.00	1.22 ± 0.40
RS EM_2					0.26 ± 0.04	0.27 ± 0.03
RS kT					< 218.4	< 218.9
PL A			$1.21^{+3.09}_{-0.79}\ 10^{-3}$	$1.86^{+4.48}_{-0.48}\ 10^{-3}$		
PL γ			$1.83^{+0.77}_{-0.60}$	2.05 ± 0.76		
RS χ^2_ν	10.53	8.236	1.087	0.826	1.327	1.330

† **MODELS** : Raymond & Smith plasma (RS), Power-law (PL). The emission measure (EM) is in units of $10^{53}\ cm^{-3}$ (based on a distance of 29.4 pc), temperature (kT_e) is given in keV, Iron abundance (Fe) is relative to solar, and the power-law slope γ is the photon index

TABLE 5. *UV fluxes (in units of $10^{-13} ergcm^{-2}s^{-1}$) for II Peg obtained in August 1989, see Table 3 for the times of each image and the A and B notation.*

Image	O I 1305	C II 1335	Si IV 1400	C IV 1550	He II 1640	Si II 1818	Si III 1897	1908
SWP36844A	3.6	3.8	–	6.0	4.9	4.3	–	–
SWP36844B	2.8	2.6	–	4.5	3.2	3.5	–	–
SWP36845A	3.9	3.8	–	7.7	2.8	3.5	–	–
SWP36845B	3.1	3.3	–	6.3	4.3	3.7	–	–
SWP36846A	3.9	5.0	–	8.5	4.2	3.6	–	–
SWP36846B	3.8	4.0	–	5.3	3.3	3.9	–	–
SWP36847A	2.9	4.0	2.6	8.1	5.4	3.5	–	–
SWP36847B	2.9	3.4	–	5.8	3.2	4.2	–	–
SWP36848A	4.4	5.2	–	8.5	4.1	5.7	–	–
SWP36848B	4.5	5.6	–	6.4	4.2	4.0	–	–
SWP36849A	5.2	5.4	–	6.2	2.8	3.3	–	–
SWP36849B	3.8	4.5	–	7.3	2.3	5.7	–	–
SWP36850A	3.5	4.7	–	5.9	5.0	3.7	–	–
SWP36850B	3.5	3.9	–	6.9	3.8	4.6	–	–
SWP36851A	3.7	4.3	–	6.9	4.2	–	–	–
SWP36851B	3.6	5.1	–	8.2	4.0	3.1	–	–
SWP36852A	3.8	3.9	–	7.5	4.7	3.6	–	–
SWP36852B	2.8	3.8	–	6.5	4.2	4.4	–	–
SWP36853A	3.2	3.9	–	7.0	2.7	3.9	–	–
SWP36853B	3.5	4.7	–	6.0	4.7	3.2	–	–
SWP36854A	3.7	4.0	1.9	6.9	3.5	3.7	–	–
SWP36854B	2.9	4.1	–	7.0	2.7	3.2	–	–
SWP36855A	6.0	9.9	9.4	29.2	7.9	8.1	2.7	1.0
SWP36855B	3.3	6.3	2.8	10.4	4.1	5.0	–	–
SWP36856A	5.2	6.2	–	9.2	5.1	5.4	–	–
SWP36856B	5.9	7.5	–	8.1	5.1	–	–	–
SWP36857	3.7	5.0	–	7.8	5.3	4.5	–	–
SWP36858A	4.2	3.5	–	5.4	2.5	6.0	–	–
SWP36858B	3.3	7.5	–	7.9	3.5	5.7	–	–
SWP36859	6.8	8.6	–	12.5	9.4	7.1	–	–
SWP36860	3.8	4.5	–	6.0	4.9	6.5	–	–
SWP36861	3.9	4.5	–	7.5	4.5	7.1	–	–
SWP36862A	3.7	4.1	–	6.4	4.2	6.5	–	–
SWP36862B	3.6	4.0	–	7.3	4.9	4.0	–	–
SWP36863A	5.3	6.8	–	4.9	4.5	5.8	–	–
SWP36863B	3.3	4.7	–	5.7	3.8	5.1	–	–

TABLE 6. *Mg II h and k fluxes (in units of $10^{-12} ergcm^{-2}s^{-1}$) for II Peg obtained in August 1989.*

Image	Mg II k 2796	Mg II h 2802
LWP16125	4.64	3.84
LWP16126	4.80	4.00
LWP16127	4.99	3.66
LWP16128	4.82	4.43
LWP16129	5.00	4.18
LWP16130	5.46	3.90
LWP16131	5.38	4.25
LWP16132	5.26	4.54
LWP16133	5.49	4.52
LWP16134	5.27	4.60
LWP16135	5.57	5.13
LWP16136	5.87	3.83
LWP16138	6.47	4.09
LWP16139	6.38	5.16
LWP16140	5.71	5.46
LWP16141	6.38	6.09
LWP16142	6.26	5.10
LWP16143	6.24	4.99
LWP16144	6.38	4.48
LWP16145	6.07	5.36

TABLE 7. *Characteristics of the U-band flares observed, where t_b and t_a are the times before and after maximum emission.*

Date	UT (max.)	Air mass	t_b (min.)	t_a (min.)	Duration (min.)	$(I_f - I_o)/I_o$	E (min.)
16 Aug	00:51	1.013	>2.56	1.08	>3.64	0.067	0.099
16 Aug	01:20	1.021	4.28	4.12	8.40	0.092	0.254
17 Aug	02:34	1.104	43.0	>5.4	>48.4	0.932	>21.4

TABLE 8. *Lines fluxes in $ergcm^{-2}s^{-1}$ for Hγ, Hδ and Ca II K during the flare of 17 August 1989. The interval from 02:09 to 02:18 UT was due to the acquiring of an arc exposure while the interval from 03:16 to 04:40 UT was due to a computer crash.*

UT	H γ	H δ	Ca II K
2:05:12	$1.64\ 10^{-11}$	$6.39\ 10^{-13}$	$4.42\ 10^{-12}$
2:09:06	$1.93\ 10^{-11}$	$2.96\ 10^{-12}$	$5.27\ 10^{-12}$
2:18:00	$2.44\ 10^{-11}$	$5.35\ 10^{-12}$	$8.76\ 10^{-12}$
2:21:54	$2.45\ 10^{-11}$	$4.79\ 10^{-12}$	$8.80\ 10^{-12}$
2:25:48	$2.39\ 10^{-11}$	$4.10\ 10^{-12}$	$8.79\ 10^{-12}$
2:29:42	$2.43\ 10^{-11}$	$4.34\ 10^{-12}$	$9.24\ 10^{-12}$
2:33:36	$2.47\ 10^{-11}$	$4.36\ 10^{-12}$	$9.43\ 10^{-12}$
2:41:00	$2.31\ 10^{-11}$	$4.59\ 10^{-12}$	$8.72\ 10^{-12}$
2:37:25	$2.36\ 10^{-11}$	$4.98\ 10^{-12}$	$8.54\ 10^{-12}$
2:48:48	$2.30\ 10^{-11}$	$4.67\ 10^{-12}$	$8.24\ 10^{-12}$
2:52:42	$2.18\ 10^{-11}$	$4.59\ 10^{-12}$	$8.08\ 10^{-12}$
2:56:36	$2.18\ 10^{-11}$	$4.54\ 10^{-12}$	$7.88\ 10^{-12}$
3:00:30	$2.14\ 10^{-11}$	$4.42\ 10^{-12}$	$7.74\ 10^{-12}$
3:04:24	$2.08\ 10^{-11}$	$4.04\ 10^{-12}$	$7.48\ 10^{-12}$
3:08:30	$1.97\ 10^{-11}$	$3.63\ 10^{-12}$	$7.22\ 10^{-12}$
3:12:36	$1.98\ 10^{-11}$	$3.38\ 10^{-12}$	$7.00\ 10^{-12}$
3:16:54	$2.00\ 10^{-11}$	$3.27\ 10^{-12}$	$7.07\ 10^{-12}$
4:40:54	$1.58\ 10^{-11}$	$5.20\ 10^{-13}$	$5.24\ 10^{-12}$
4:44:36	$1.60\ 10^{-11}$	$8.95\ 10^{-13}$	$5.32\ 10^{-12}$
4:48:24	$1.58\ 10^{-11}$	$4.01\ 10^{-13}$	$5.19\ 10^{-12}$
4:52:00	$1.55\ 10^{-11}$	$3.81\ 10^{-13}$	$4.93\ 10^{-12}$
4:56:48	$1.53\ 10^{-11}$	$2.24\ 10^{-13}$	$4.97\ 10^{-12}$
5:00:24	$1.59\ 10^{-11}$	$4.74\ 10^{-13}$	$4.91\ 10^{-12}$
5:04:18	$1.53\ 10^{-11}$	$4.21\ 10^{-13}$	$5.03\ 10^{-12}$
5:08:12	$1.51\ 10^{-11}$	$3.95\ 10^{-13}$	$5.16\ 10^{-12}$
5:12:06	$1.60\ 10^{-11}$	$3.29\ 10^{-13}$	$5.11\ 10^{-12}$
5:20:00	$1.60\ 10^{-11}$	$9.79\ 10^{-13}$	$5.45\ 10^{-12}$
5:24:06	$1.69\ 10^{-11}$	$1.68\ 10^{-12}$	$5.95\ 10^{-12}$
5:28:12	$1.70\ 10^{-11}$	$1.90\ 10^{-12}$	$6.27\ 10^{-12}$
5:32:18	$1.71\ 10^{-11}$	$1.63\ 10^{-12}$	$6.05\ 10^{-12}$
5:36:24	$1.70\ 10^{-11}$	$1.32\ 10^{-12}$	$6.11\ 10^{-12}$
5:40:30	$1.66\ 10^{-11}$	$1.25\ 10^{-12}$	$5.92\ 10^{-12}$
5:44:36	$1.69\ 10^{-11}$	$1.36\ 10^{-12}$	$5.84\ 10^{-12}$
5:48:42	$1.62\ 10^{-11}$	$1.05\ 10^{-12}$	$5.77\ 10^{-12}$
5:52:48	$1.68\ 10^{-11}$	$1.05\ 10^{-12}$	$5.91\ 10^{-12}$
5:56:54	$1.65\ 10^{-11}$	$8.41\ 10^{-13}$	$5.59\ 10^{-12}$
6:03:00	$1.72\ 10^{-11}$	$9.85\ 10^{-13}$	$5.67\ 10^{-12}$

TABLE 9. *Lines fluxes in $ergcm^{-2}s^{-1}$ for Hα during the flare of 17 August 1989. The interval from 02:11 to 02:20 UT was due to the acquiring of an arc exposure while the interval from 03:19 to 04:39 UT was due to a computer crash.*

UT	H α	UT	H α
2:07:24	$6.09\ 10^{-12}$	4:39:12	$6.02\ 10^{-12}$
2:11:18	$1.06\ 10^{-11}$	4:43:00	$5.95\ 10^{-12}$
2:20:12	$1.11\ 10^{-11}$	4:46:42	$5.95\ 10^{-12}$
2:24:06	$1.12\ 10^{-11}$	4:50:30	$5.34\ 10^{-12}$
2:28:00	$1.10\ 10^{-11}$	4:54:12	$5.65\ 10^{-12}$
2:31:54	$1.23\ 10^{-11}$	4:58:42	$5.28\ 10^{-12}$
2:35:48	$1.11\ 10^{-11}$	5:02:36	$5.08\ 10^{-12}$
2:43:12	$1.14\ 10^{-11}$	5:06:30	$5.19\ 10^{-12}$
2:47:06	$1.11\ 10^{-11}$	5:10:24	$5.38\ 10^{-12}$
2:51:00	$1.09\ 10^{-11}$	5:14:18	$5.43\ 10^{-12}$
2:54:54	$1.10\ 10^{-11}$	5:22:18	$7.23\ 10^{-12}$
2:58:48	$1.09\ 10^{-11}$	5:26:24	$8.59\ 10^{-12}$
3:02:42	$1.03\ 10^{-11}$	5:30:29	$8.07\ 10^{-12}$
3:06:42	$1.02\ 10^{-11}$	5:34:36	$7.91\ 10^{-12}$
3:10:48	$9.98\ 10^{-12}$	5:38:54	$7.41\ 10^{-12}$
3:15:00	$9.71\ 10^{-12}$	5:42:48	$7.19\ 10^{-12}$
3:19:18	$9.44\ 10^{-12}$	5:46:54	$7.27\ 10^{-12}$
		5:51:00	$7.04\ 10^{-12}$
		5:55:06	$6.69\ 10^{-12}$

TABLE 10. *LAC spectral fit parameters for the X-ray flare of August 17 on II Peg, also indicated are 1σ error ranges.*

time (sec)	LAC ($ct\,s^{-1}$)	1σ	EM ($10^{53}\,cm^{-3}$)	1σ	T($10^7\,K$)	1σ
0	110.9	1.7	25.1	1.0	6.6	0.6
64	108.4	1.7	24.3	1.0	6.3	0.6
128	105.9	1.7	23.3	1.0	6.3	0.7
192	103.9	1.6	24.0	1.0	6.0	0.8
256	99.0	1.6	23.0	1.0	5.8	0.6
320	98.1	1.6	22.8	1.0	6.1	0.6
384	92.8	1.5	22.1	0.9	5.6	0.6
448	92.5	1.5	22.2	1.0	5.5	0.5
512	87.4	1.5	21.2	1.0	5.0	0.5
576	87.4	1.5	21.0	0.9	5.5	0.5
640	84.8	1.5	21.3	1.0	5.0	0.5
704	81.4	1.5	19.3	0.9	5.5	0.6
768	71.7	1.5	19.8	1.0	4.2	0.4
832	75.7	1.4	18.6	0.9	5.4	0.6
896	70.9	1.4	17.9	0.9	4.8	0.5
960	67.7	1.4	17.2	0.9	5.1	0.6
1024	68.3	1.4	18.2	1.0	4.4	0.4
1088	66.1	1.4	17.2	1.0	4.8	0.5
1152	63.6	1.4	16.4	1.0	4.7	0.5
1216	62.8	1.4	16.0	0.9	5.0	0.6
1280	61.5	1.3	16.7	1.0	4.4	0.5
1344	59.5	1.3	16.0	1.0	4.4	0.5
1408	56.5	1.3	15.1	0.9	4.3	0.5
1472	54.3	1.3	14.7	0.9	4.2	0.5
1536	53.8	1.3	15.0	1.0	4.1	0.5
1600	51.4	1.3	14.4	1.0	4.0	0.5
1664	52.1	1.3	13.8	0.9	4.7	0.6
1728	50.3	1.3	13.6	0.9	4.1	0.5
1792	48.9	1.3	14.0	0.9	3.9	0.5

TABLE 11. *The range of integrated flare energies for possible values of β from 0.1 to 5. t_d is the exponential decay time, as defined by Eq. (3), of the X-ray light curve, L_x the integrated flare energy in erg.*

β	t_d (hrs.)	L_x (erg)
0.10	0.5446	$2.678\ 10^{35}$
0.25	0.5020	$2.463\ 10^{35}$
0.50	0.4442	$2.194\ 10^{35}$
0.75	0.3984	$1.996\ 10^{35}$
1.00	0.3611	$1.843\ 10^{35}$
1.25	0.3302	$1.720\ 10^{35}$
1.50	0.3041	$1.619\ 10^{35}$
1.75	0.2819	$1.534\ 10^{35}$
2.00	0.2627	$1.462\ 10^{35}$
2.25	0.2459	$1.400\ 10^{35}$
2.50	0.2312	$1.345\ 10^{35}$
2.75	0.2181	$1.297\ 10^{35}$
3.00	0.2064	$1.254\ 10^{35}$
3.25	0.1959	$1.214\ 10^{35}$
3.50	0.1864	$1.179\ 10^{35}$
4.00	0.1699	$1.118\ 10^{35}$
5.00	0.1444	$1.022\ 10^{35}$

TABLE A1. *Photometric data on the Vilnius UPXYZVS system for II Peg and the comparison star HD 224016 for the 15 August 1989. The data were obtained from Maidanak* (long = $4^h27^m36^s$, lat = $38^\circ 41' 03''$), *time is given in Local Sidereal Time.*

LST	V	U-V	P-V	X-V	Y-V	Z-V	S-V		LST	V	U-V	P-V	X-V	Y-V	Z-V	S-V	
202500	8.485	2.983	2.504	1.663	0.621	0.267	0.615	comp	212659	7.512	3.458	2.906	2.047	0.769	0.375	0.856	
203339	7.492	3.517	2.915	2.051	0.777	0.413	0.838		212816	7.492	3.499	2.954	2.040	0.782	0.407	0.836	
203452	7.485	3.473	2.946	2.067	0.761	0.399	0.838		212856	7.488	3.487	2.935	2.083	0.784	0.404	0.836	
203611	7.486	3.491	2.964	2.055	0.784	0.409	0.845		212940	7.491	3.496	2.958	2.066	0.780	0.407	0.843	
203710	7.484	3.508	2.982	2.076	0.792	0.420	0.835		213020	7.485	3.530	2.922	2.047	0.793	0.460	0.839	
203920	7.483	3.487	2.957	2.057	0.786	0.396	0.847		213059	7.507	3.448	2.909	2.036	0.768	0.380	0.859	
204020	7.484	3.490	2.933	2.055	0.790	0.414	0.840		213140	7.508	3.461	2.910	2.029	0.772	0.365	0.872	
204220	7.492	3.475	2.936	2.034	0.769	0.400	0.848		213220	7.493	3.522	2.923	2.042	0.786	0.396	0.833	
204318	7.476	3.489	2.953	2.072	0.805	0.358	0.829		213301	7.489	3.482	2.937	2.059	0.780	0.389	0.834	
204440	7.484	3.531	2.943	2.077	0.771	0.407	0.837		213342	7.503	3.473	2.912	2.055	0.775	0.390	0.843	
204552	7.481	3.497	2.965	2.066	0.798	0.406	0.841		213426	7.498	3.475	2.932	2.053	0.783	0.406	0.846	
204702	7.514	3.499	2.927	2.027	0.751	0.373	0.872		213542	7.478	3.470	2.945	2.072	0.737	0.405	0.835	
204745	7.510	3.471	2.927	2.059	0.753	0.379	0.868		213700	8.503	2.955	2.476	1.650	0.611	0.258	0.625	comp
204840	7.483	3.503	2.949	2.070	0.797	0.411	0.846		213854	7.478	3.525	2.983	2.069	0.808	0.420	0.816	
204928	7.488	3.491	2.955	2.059	0.796	0.403	0.840		213934	7.487	3.471	2.958	2.052	0.790	0.396	0.833	
205044	7.486	3.493	2.947	2.042	0.787	0.398	0.828		214018	7.486	3.491	2.944	2.062	0.802	0.417	0.825	
205125	7.507	3.556	2.938	2.074	0.761	0.390	0.862		214102	7.509	3.484	2.938	2.042	0.777	0.383	0.850	
205211	7.496	3.501	2.967	2.043	0.789	0.402	0.853		214143	7.495	3.490	2.931	2.080	0.786	0.409	0.845	
205408	7.479	3.481	2.959	2.066	0.793	0.408	0.832		214228	7.511	3.494	2.924	2.068	0.783	0.394	0.855	
205455	7.506	3.473	2.918	2.050	0.765	0.379	0.846		214302	7.507	3.508	2.946	2.074	0.779	0.395	0.860	
205537	7.489	3.478	2.972	2.070	0.798	0.405	0.834		214349	7.503	3.508	2.974	2.080	0.787	0.388	0.836	
205621	7.482	3.474	2.932	2.058	0.781	0.411	0.825		214432	7.511	3.501	2.941	2.040	0.777	0.395	0.851	
205705	7.500	3.533	2.934	2.042	0.773	0.388	0.849		214518	7.518	3.507	2.944	2.035	0.765	0.398	0.843	
205747	7.478	3.503	2.951	2.097	0.799	0.415	0.813		214626	7.497	3.494	2.925	2.046	0.771	0.389	0.840	
205830	7.480	3.492	2.929	2.060	0.794	0.407	0.824		214707	7.486	3.502	2.930	2.046	0.784	0.402	0.839	
205921	7.500	3.488	2.932	2.039	0.784	0.395	0.842		214750	7.494	3.477	2.950	2.054	0.786	0.395	0.839	
210004	7.497	3.508	2.937	2.079	0.794	0.434	0.853		214833	7.485	3.481	2.921	2.047	0.793	0.397	0.838	
211200	8.495	2.964	2.489	1.651	0.616	0.265	0.622	comp	214915	7.499	3.479	2.942	2.013	0.781	0.401	0.860	
211340	7.473	3.506	2.965	2.072	0.802	0.422	0.828		214956	7.485	3.495	2.976	2.078	0.794	0.397	0.835	
211630	7.489	3.491	2.932	2.063	0.779	0.383	0.839		215038	7.497	3.471	2.925	2.054	0.766	0.394	0.846	
211714	7.488	3.500	2.857	2.070	0.772	0.387	0.832		215121	7.478	3.480	2.942	2.071	0.794	0.397	0.826	
211802	7.480	3.481	2.961	2.063	0.799	0.420	0.824		215203	7.487	3.461	2.942	2.067	0.794	0.413	0.840	
211842	7.510	3.449	2.913	2.052	0.763	0.369	0.845		215600	8.513	2.948	2.467	1.649	0.602	0.253	0.632	comp
211938	7.495	3.487	2.937	2.084	0.793	0.406	0.852		222053	7.488	3.545	2.934	2.062	0.792	0.409	0.829	
212017	7.484	3.516	2.956	2.035	0.781	0.406	0.832		222113	7.511	3.523	2.947	2.057	0.787	0.407	0.844	
212104	7.488	3.479	2.934	2.043	0.799	0.400	0.821		222219	7.528	3.514	2.938	2.056	0.783	0.382	0.854	
212230	7.489	3.479	2.912	2.074	0.777	0.392	0.845		222303	7.528	3.701	3.099	2.132	0.916	0.421	0.848	
212319	7.473	3.513	2.958	2.076	0.798	0.409	0.822		222455	7.503	3.528	2.950	2.060	0.789	0.404	0.851	
212414	7.490	3.470	2.941	2.057	0.792	0.407	0.840		222538	7.480	3.543	3.002	2.065	0.808	0.409	0.835	
212456	7.488	3.501	2.957	2.058	0.809	0.397	0.832		222621	7.505	3.511	2.924	2.056	0.780	0.398	0.854	
212536	7.496	3.506	2.970	2.061	0.782	0.420	0.839		222704	7.503	3.518	2.931	2.017	0.783	0.377	0.861	
212618	7.516	3.467	2.910	2.044	0.758	0.375	0.865		222747	7.510	3.502	3.028	2.042	0.758	0.389	0.865	

TABLE A1. *(continued)*

LST	V	U-V	P-V	X-V	Y-V	Z-V	S-V		LST	V	U-V	P-V	X-V	Y-V	Z-V	S-V	
222837	7.489	3.483	2.960	2.080	0.787	0.408	0.835		231525	7.481	3.471	2.945	2.063	0.788	0.418	0.824	
222920	7.487	3.513	2.957	2.071	0.795	0.398	0.835		231637	7.478	3.482	2.962	2.042	0.794	0.411	0.826	
223000	7.511	3.483	2.941	2.033	0.777	0.378	0.866		231717	7.498	3.443	2.921	2.032	0.771	0.398	0.850	
223043	7.498	3.525	2.946	2.062	0.782	0.394	0.836		231756	7.495	3.468	2.912	2.037	0.778	0.386	0.854	
223138	7.481	3.515	2.985	2.070	0.802	0.409	0.822		231837	7.484	3.462	2.913	2.058	0.780	0.405	0.838	
223303	7.505	3.522	2.930	2.056	0.775	0.388	0.854		231918	7.475	3.507	2.930	2.060	0.797	0.419	0.820	
223346	7.508	3.460	2.924	2.045	0.766	0.391	0.849		232002	7.486	3.506	2.957	2.063	0.788	0.405	0.813	
223428	7.498	3.521	2.934	2.079	0.772	0.403	0.834		232045	7.488	3.462	2.935	2.048	0.784	0.403	0.826	
223512	7.480	3.537	2.980	2.108	0.806	0.423	0.809		232125	7.476	3.491	2.962	2.038	0.791	0.410	0.828	
223602	7.546	3.583	2.980	2.074	0.818	0.382	0.857		232206	7.492	3.495	2.972	2.047	0.771	0.400	0.838	
223808	7.505	3.511	2.965	2.051	0.786	0.382	0.852		232329	7.481	3.497	2.940	2.056	0.799	0.409	0.830	
223850	7.496	3.517	2.930	2.071	0.785	0.412	0.844		232410	7.490	3.442	2.926	2.052	0.782	0.393	0.845	
223936	7.499	3.524	2.939	2.071	0.790	0.404	0.834		232451	7.495	3.490	2.947	2.044	0.784	0.408	0.837	
224100	8.500	2.976	2.491	1.652	0.614	0.266	0.619	comp	232532	7.481	3.502	2.954	2.063	0.805	0.411	0.829	
224257	7.482	3.552	2.970	2.094	0.821	0.427	0.812		232622	7.484	3.464	2.955	2.060	0.792	0.413	0.825	
224341	7.496	3.512	2.966	2.077	0.787	0.415	0.840		232702	7.480	3.508	2.967	2.058	0.802	0.410	0.828	
224430	7.514	3.533	2.946	2.039	0.783	0.381	0.863		232749	7.485	3.484	2.978	2.056	0.787	0.414	0.839	
224508	7.506	3.531	2.929	2.056	0.782	0.397	0.846		232834	7.493	3.504	2.926	2.068	0.785	0.406	0.842	
224552	7.530	3.502	2.960	2.044	0.764	0.389	0.857		232920	7.493	3.512	2.951	2.065	0.777	0.399	0.846	
224634	7.503	3.553	2.946	2.062	0.794	0.411	0.839		232959	7.503	3.492	2.932	2.028	0.759	0.386	0.854	
224715	7.508	3.463	2.922	2.020	0.771	0.399	0.843		233046	7.497	3.502	2.927	2.041	0.789	0.395	0.849	
224815	7.470	3.524	2.978	2.050	0.799	0.398	0.812		233140	8.511	2.977	2.499	1.653	0.620	0.274	0.622	comp
224934	7.495	3.469	2.934	2.032	0.762	0.398	0.837		233226	7.478	3.518	2.940	2.051	0.796	0.414	0.839	
225058	7.486	3.492	2.750	2.067	0.775	0.381	0.834		233301	7.491	3.466	2.921	2.037	0.777	0.403	0.834	
225147	7.475	3.485	2.959	2.072	0.789	0.412	0.829		233343	7.485	3.497	2.969	2.049	0.782	0.413	0.844	
225228	7.471	3.528	2.947	2.061	0.799	0.420	0.819		233436	7.481	3.471	2.940	2.037	0.777	0.425	0.827	
225309	7.476	3.472	2.955	2.041	0.796	0.422	0.823		233524	7.481	3.495	2.926	2.049	0.797	0.413	0.836	
225424	7.494	3.472	2.906	2.040	0.786	0.396	0.850		233607	7.498	3.465	2.921	2.026	0.770	0.399	0.843	
225508	7.482	3.512	2.935	2.048	0.792	0.393	0.825		233647	7.483	3.469	2.964	2.028	0.773	0.399	0.828	
225547	7.497	3.521	2.930	2.049	0.770	0.389	0.843		233727	7.489	3.474	2.923	2.042	0.785	0.415	0.838	
225628	7.488	3.506	2.933	2.066	0.787	0.401	0.835		233808	7.489	3.470	2.915	2.055	0.765	0.403	0.844	
225710	7.483	3.490	2.927	2.044	0.779	0.412	0.823		233853	7.490	3.480	2.936	2.028	0.782	0.403	0.844	
225754	7.480	3.520	2.959	2.073	0.790	0.410	0.837		234034	7.494	3.441	2.908	2.040	0.781	0.396	0.833	
225837	7.477	3.519	2.953	2.063	0.798	0.414	0.831		234113	7.491	3.514	2.947	2.025	0.774	0.397	0.833	
225936	7.458	3.502	2.948	2.059	0.810	0.430	0.824		234154	7.482	3.493	2.944	2.071	0.788	0.418	0.836	
230025	7.485	3.531	2.936	2.040	0.791	0.412	0.835		234236	7.473	3.448	2.926	2.029	0.779	0.420	0.826	
230500	8.509	2.963	2.488	1.650	0.613	0.258	0.621	comp	234316	7.474	3.468	2.942	2.049	0.789	0.403	0.832	
231033	7.494	3.449	2.939	2.039	0.768	0.399	0.839		234357	7.471	3.499	2.944	2.038	0.786	0.414	0.827	
231118	7.480	3.511	2.978	2.043	0.786	0.417	0.830		234437	7.465	3.523	2.929	2.053	0.800	0.435	0.818	
231150	7.493	3.477	2.941	2.029	0.765	0.399	0.844		001900	8.515	2.987	2.509	1.662	0.626	0.277	0.625	comp
231239	7.506	3.495	2.919	2.027	0.766	0.390	0.853		002541	7.494	3.536	3.001	2.063	0.797	0.439	0.832	
231319	7.492	3.500	2.937	2.048	0.772	0.387	0.833		002541	7.494	3.536	3.001	2.063	0.797	0.439	0.832	
231402	7.491	3.491	2.930	2.043	0.782	0.408	0.846		002630	7.487	3.534	2.962	2.085	0.808	0.425	0.825	
231443	7.488	3.479	2.935	2.058	0.776	0.407	0.849		002713	7.499	3.511	2.973	2.075	0.795	0.411	0.830	

TABLE A1. *(continued)*

LST	V	U-V	P-V	X-V	Y-V	Z-V	S-V	
002753	7.497	3.507	3.015	2.064	0.816	0.418	0.828	
002837	7.492	3.533	2.978	2.064	0.794	0.425	0.829	
002918	7.506	3.521	2.963	2.043	0.792	0.451	0.834	
003001	7.515	3.516	2.954	2.053	0.780	0.401	0.842	
003041	7.512	3.519	2.986	2.055	0.778	0.399	0.844	
003121	7.508	3.566	2.989	2.038	0.790	0.402	0.840	
003202	7.501	3.548	2.971	2.081	0.807	0.423	0.830	
003242	7.510	3.522	2.972	2.061	0.798	0.411	0.841	
003446	7.507	3.574	2.976	2.055	0.782	0.377	0.829	
003526	7.512	3.566	2.951	2.065	0.779	0.400	0.843	
003611	7.501	3.511	2.969	2.064	0.801	0.411	0.824	
003651	7.500	3.541	2.995	2.060	0.801	0.410	0.819	
003740	7.501	3.543	3.001	2.085	0.797	0.435	0.831	
003820	7.519	3.521	2.978	2.095	0.784	0.394	0.848	
003859	7.492	3.570	3.014	2.080	0.816	0.434	0.814	
003930	7.500	3.573	2.986	2.100	0.791	0.422	0.820	
004026	7.520	3.504	2.989	2.057	0.784	0.391	0.850	
004106	7.536	3.493	2.948	2.054	0.771	0.378	0.862	
004237	7.506	3.581	2.973	2.100	0.801	0.399	0.831	
004318	7.519	3.539	2.964	2.081	0.785	0.409	0.845	
004438	7.507	3.544	2.984	2.077	0.797	0.418	0.844	
004528	7.512	3.539	2.947	2.071	0.794	0.418	0.856	
004611	7.523	3.558	2.976	2.044	0.790	0.388	0.842	
004657	7.515	3.545	3.012	2.093	0.798	0.395	0.843	
004739	7.513	3.558	3.008	2.081	0.804	0.420	0.827	
004828	7.508	3.552	3.006	2.085	0.803	0.425	0.829	
004957	7.527	3.547	2.984	2.079	0.786	0.444	0.845	
005039	7.521	3.552	2.977	2.047	0.802	0.398	0.820	
005123	7.519	3.560	2.980	2.085	0.806	0.409	0.849	
005201	7.526	3.558	2.977	2.071	0.789	0.401	0.845	
005246	7.507	3.584	2.987	2.060	0.791	0.411	0.827	
005325	7.513	3.578	3.018	2.083	0.788	0.401	0.829	
005406	7.521	3.572	2.984	2.074	0.790	0.413	0.849	
005446	7.521	3.566	3.000	2.094	0.787	0.404	0.846	
005705	7.528	3.550	2.996	2.074	0.783	0.400	0.844	
005751	7.535	3.577	2.994	2.102	0.776	0.403	0.855	
005834	7.540	3.574	2.959	2.061	0.783	0.396	0.859	
005916	7.527	3.562	3.005	2.092	0.802	0.423	0.843	
005957	7.518	3.561	3.000	2.090	0.784	0.420	0.831	
010037	7.541	3.548	2.980	2.042	0.775	0.370	0.849	
010118	7.548	3.556	2.972	2.077	0.768	0.386	0.870	
010202	7.517	3.618	3.002	2.083	0.805	0.426	0.831	
010246	7.529	3.550	2.966	2.087	0.796	0.411	0.849	
010700	8.571	3.051	2.535	1.675	0.624	0.268	0.633	comp

TABLE A2. *Photometric data on the Vilnius UPXYZVS system for II Peg and the comparison star HD 224016 for the 16 August 1989. The data were obtained from Maidanak* (long = $4^h27^m36^s$, lat = $38^\circ 41' 03''$), *time is given in Local Sidereal Time.*

LST	V	U-V	P-V	X-V	Y-V	Z-V	S-V	
195800	8.472	2.948	2.478	1.630	0.609	0.263	0.639	comp.
200133	7.335	3.465	2.919	2.053	0.773	0.402	0.848	
200213	7.339	3.445	2.913	2.042	0.768	0.391	0.846	
200255	7.335	3.455	2.908	2.056	0.782	0.390	0.843	
200335	7.346	3.484	2.937	2.043	0.761	0.390	0.854	
200418	7.352	3.464	2.932	2.034	0.757	0.384	0.860	
200601	7.339	3.455	2.922	2.037	0.762	0.374	0.850	
200641	7.339	3.441	2.942	2.014	0.768	0.393	0.843	
200723	7.329	3.500	2.910	2.036	0.784	0.407	0.830	
200802	7.331	3.461	2.880	2.038	0.795	0.394	0.835	
200844	7.344	3.475	2.917	2.000	0.766	0.377	0.833	
200933	7.350	3.464	2.898	2.040	0.762	0.378	0.851	
201048	7.333	3.459	2.903	2.057	0.782	0.380	0.850	
201130	7.331	3.487	2.937	2.042	0.780	0.382	0.834	
201211	7.321	3.493	2.926	2.042	0.783	0.388	0.831	
201253	7.336	3.438	2.946	2.024	0.781	0.380	0.842	
201333	7.341	3.479	2.903	2.028	0.775	0.382	0.825	
201415	7.346	3.420	2.893	2.050	0.773	0.389	0.840	
201456	7.337	3.457	2.910	2.052	0.768	0.379	0.839	
201539	7.331	3.454	2.925	2.031	0.780	0.380	0.844	
201655	7.314	3.496	2.952	2.068	0.788	0.408	0.829	
201737	7.346	3.388	2.913	2.020	0.777	0.374	0.854	
201836	7.336	3.457	2.901	2.032	0.765	0.375	0.846	
201919	7.335	3.449	2.887	2.034	0.766	0.393	0.828	
201958	7.342	3.439	2.903	2.022	0.773	0.365	0.828	
202038	7.337	3.432	2.896	2.013	0.783	0.402	0.843	
202119	7.344	3.427	2.921	2.019	0.764	0.369	0.849	
202256	7.325	3.462	2.959	2.060	0.781	0.409	0.836	
202336	7.335	3.484	2.915	2.023	0.777	0.377	0.839	
202416	7.342	3.463	2.909	2.035	0.763	0.360	0.843	
202500	7.348	3.442	2.920	2.020	0.761	0.376	0.849	
202542	7.356	3.462	2.919	2.019	0.757	0.368	0.850	
202623	7.342	3.461	2.885	2.038	0.757	0.387	0.833	
202705	7.335	3.514	2.919	2.012	0.777	0.391	0.847	
203100	8.484	2.964	2.490	1.644	0.613	0.257	0.636	comp.
205000	8.493	2.962	2.477	1.634	0.604	0.250	0.634	comp.
205624	7.331	3.468	2.917	2.022	0.770	0.400	0.813	
205712	7.342	3.477	2.907	2.000	0.775	0.376	0.836	
205753	7.340	3.452	2.897	2.014	0.792	0.371	0.834	
205833	7.338	3.477	2.941	2.042	0.781	0.401	0.827	
205914	7.347	3.492	2.910	2.060	0.781	0.380	0.827	

TABLE A2. *(continued)*

LST	V	U-V	P-V	X-V	Y-V	Z-V	S-V		LST	V	U-V	P-V	X-V	Y-V	Z-V	S-V	
205953	7.340	3.454	2.938	2.047	0.784	0.391	0.828		213311	7.347	3.464	2.900	2.027	0.784	0.384	0.821	
210103	7.356	3.463	2.910	2.042	0.774	0.369	0.840		213542	7.370	3.438	2.667	2.014	0.748	0.363	0.847	
210143	7.345	3.448	2.903	2.052	0.773	0.389	0.839		213625	7.347	3.490	2.920	2.045	0.793	0.397	0.830	
210224	7.344	3.459	2.917	2.039	0.793	0.376	0.830		213704	7.365	3.452	2.910	2.023	0.784	0.384	0.845	
210304	7.351	3.470	2.888	2.023	0.765	0.386	0.845		213748	7.360	3.469	2.913	2.031	0.772	0.399	0.825	
210345	7.348	3.464	2.925	2.027	0.768	0.394	0.824		213829	7.362	3.496	2.894	2.033	0.788	0.395	0.837	
210426	7.362	3.451	2.925	2.035	0.754	0.372	0.851		213949	7.367	3.479	2.923	2.032	0.770	0.383	0.841	
210507	7.357	3.421	2.888	2.006	0.770	0.379	0.841		214021	7.361	3.513	2.945	2.057	0.787	0.385	0.831	
210548	7.349	3.464	2.910	2.061	0.782	0.399	0.836		214148	7.344	3.477	2.909	2.036	0.803	0.399	0.822	
210628	7.357	3.438	2.937	2.001	0.768	0.392	0.825		214230	7.356	3.425	2.959	2.036	0.778	0.374	0.837	
210744	7.345	3.478	2.939	2.053	0.775	0.386	0.844		214309	7.359	3.463	2.895	2.025	0.787	0.387	0.830	
210824	7.336	3.512	2.956	2.037	0.782	0.401	0.819		214357	7.371	3.454	2.910	2.027	0.768	0.382	0.840	
210904	7.343	3.460	2.935	2.051	0.782	0.384	0.821		214440	7.366	3.488	2.922	2.007	0.756	0.493	0.828	
210944	7.356	3.466	2.916	2.009	0.774	0.392	0.842		214520	7.368	3.467	2.912	2.044	0.777	0.490	0.848	
211023	7.345	3.460	2.920	2.010	0.773	0.393	0.827		214604	7.352	3.479	2.928	2.036	0.776	0.504	0.827	
211105	7.350	3.459	2.931	2.040	0.779	0.398	0.838		214646	7.354	3.477	2.908	2.041	0.781	0.492	0.841	
211154	7.355	3.465	2.897	2.021	0.774	0.378	0.844		214825	7.353	3.462	2.931	2.045	0.775	0.502	0.831	
211234	7.349	3.482	2.953	2.043	0.772	0.382	0.826		214905	7.354	3.456	2.930	2.037	0.779	0.489	0.841	
211339	7.353	3.458	2.924	2.017	0.765	0.386	0.834		214955	7.344	3.508	2.922	2.061	0.794	0.510	0.816	
211435	7.348	3.442	2.935	2.027	0.777	0.392	0.826		215041	7.361	3.477	2.939	2.018	0.782	0.497	0.826	
211516	7.345	3.480	2.932	2.050	0.780	0.391	0.830		215124	7.360	3.454	2.925	2.018	0.768	0.483	0.838	
211558	7.349	3.459	2.914	2.034	0.768	0.400	0.833		215257	7.344	3.501	2.940	2.037	0.790	0.499	0.819	
211638	7.339	3.483	2.951	2.044	0.787	0.395	0.825		215257	7.348	3.478	2.958	2.045	0.778	0.485	0.833	
211732	7.337	3.469	2.933	2.023	0.798	0.403	0.819		215337	7.348	3.458	2.921	2.051	0.787	0.506	0.819	
211820	7.358	3.654	2.933	2.024	0.766	0.388	0.842		215800	8.511	2.977	2.494	1.655	0.616	0.365	0.631	comp.
211901	7.355	3.463	2.902	2.000	0.787	0.379	0.837		222300	8.529	3.004	2.522	1.656	0.617	0.339	0.637	comp.
211940	7.349	3.521	2.905	1.999	0.784	0.384	0.842		222853	7.386	3.473	2.929	2.036	0.771	0.432	0.846	
212124	7.340	3.501	2.932	2.032	0.786	0.408	0.820		222935	7.371	3.497	2.927	2.058	0.788	0.465	0.821	
212213	7.347	3.509	2.917	2.053	0.777	0.395	0.835		223019	7.368	3.513	2.943	2.054	0.790	0.468	0.832	
212253	7.355	3.464	2.910	2.003	0.785	0.389	0.843		223104	7.373	3.511	2.937	2.029	0.782	0.460	0.828	
212332	7.344	3.489	2.891	2.023	0.792	0.403	0.835		223143	7.380	3.515	2.941	2.044	0.782	0.457	0.831	
212413	7.348	3.483	2.913	2.039	0.772	0.399	0.815		223224	7.359	3.555	2.966	2.065	0.796	0.458	0.808	
212457	7.344	3.476	2.912	2.041	0.774	0.398	0.833		223303	7.394	3.513	2.909	2.054	0.775	0.431	0.847	
212548	7.362	3.479	2.897	2.039	0.767	0.374	0.849		223344	7.378	3.496	2.943	2.075	0.777	0.444	0.831	
212700	8.500	2.970	2.484	1.647	0.610	0.277	0.633	comp.	223425	7.370	3.526	2.961	2.054	0.794	0.454	0.824	
212847	7.346	3.451	2.912	2.070	0.784	0.384	0.834		223505	7.401	3.503	2.928	2.021	0.769	0.434	0.833	
212926	7.360	3.465	2.890	2.033	0.777	0.391	0.842		223651	7.370	3.519	2.943	2.072	0.786	0.446	0.828	
213009	7.337	3.501	2.921	2.038	0.818	0.405	0.812		223732	7.376	3.516	2.914	2.048	0.795	0.453	0.828	
213049	7.380	3.459	2.867	2.010	0.741	0.375	0.857		223819	7.392	3.503	2.933	2.030	0.768	0.421	0.848	
213145	7.349	3.474	2.924	2.011	0.785	0.393	0.837		223900	7.388	3.523	2.922	2.018	0.762	0.427	0.846	
213231	7.355	3.460	2.925	2.009	0.780	0.390	0.846		223945	7.373	3.544	2.944	2.051	0.789	0.429	0.835	

TABLE A2. *(continued)*

LST	V	U-V	P-V	X-V	Y-V	Z-V	S-V	
224115	7.404	3.507	2.939	2.015	0.769	0.412	0.851	
224157	7.363	3.517	2.974	2.049	0.796	0.461	0.810	
224338	7.359	3.555	2.939	2.057	0.806	0.452	0.822	
224419	7.375	3.550	2.907	2.050	0.793	0.432	0.837	
224508	7.390	3.500	2.950	2.030	0.795	0.418	0.855	
224556	7.378	3.518	2.936	2.044	0.790	0.426	0.833	
224637	7.393	3.525	2.909	2.034	0.760	0.405	0.852	
224721	7.399	3.519	2.940	2.023	0.766	0.402	0.859	
224800	7.377	3.527	2.948	2.060	0.787	0.422	0.837	
224843	7.377	3.544	2.940	2.047	0.786	0.414	0.836	
224950	7.377	3.513	2.968	2.065	0.794	0.415	0.825	
225031	7.389	3.521	2.947	2.038	0.780	0.400	0.836	
225116	7.376	3.519	2.945	2.054	0.787	0.424	0.827	
225159	7.381	3.512	2.923	2.048	0.787	0.417	0.845	
225240	7.368	3.533	2.952	2.037	0.790	0.420	0.822	
225334	7.388	3.500	2.936	2.033	0.775	0.405	0.826	
225415	7.364	3.521	2.958	2.060	0.799	0.422	0.834	
225457	7.381	3.515	2.958	2.041	0.775	0.405	0.838	
225538	7.380	3.499	2.942	2.046	0.770	0.400	0.830	
225620	7.378	3.500	2.930	2.037	0.791	0.420	0.845	
225700	8.531	3.022	2.534	1.666	1.620	0.300	0.632	comp.
225826	7.372	3.524	2.951	2.066	0.797	0.406	0.828	
225908	7.379	3.541	2.958	2.060	0.787	0.410	0.833	
225949	7.380	3.524	2.931	2.043	0.791	0.388	0.838	
230036	7.381	3.537	2.936	2.030	0.784	0.399	0.839	
230116	7.392	3.539	2.922	2.052	0.773	0.376	0.847	
230157	7.377	3.538	2.947	2.076	0.777	0.394	0.832	
230243	7.369	3.547	2.981	2.066	0.795	0.433	0.825	
230325	7.380	3.524	2.954	2.168	0.797	0.423	0.836	
230407	7.379	3.514	2.947	2.035	0.784	0.410	0.831	
230454	7.386	3.518	2.954	2.053	0.779	0.401	0.845	
230613	7.384	3.539	2.960	2.053	0.767	0.417	0.839	
230654	7.388	3.530	2.955	2.044	0.785	0.406	0.833	
230737	7.391	3.523	2.973	2.065	0.774	0.411	0.846	
230822	7.383	3.528	2.934	2.041	0.797	0.408	0.837	
230906	7.383	3.508	2.946	2.039	0.783	0.420	0.836	
230948	7.383	3.552	2.942	2.055	0.787	0.409	0.835	
231029	7.394	3.546	2.964	2.026	0.772	0.409	0.846	
231146	7.381	3.499	2.957	2.050	0.788	0.421	0.829	
231228	7.382	3.525	2.944	2.075	0.782	0.419	0.833	
231309	7.382	3.530	2.954	2.057	0.786	0.426	0.825	
231353	7.389	3.487	2.959	2.057	0.783	0.409	0.815	
231434	7.385	3.506	2.977	2.054	0.784	0.397	0.838	
231515	7.392	3.504	2.940	2.027	0.784	0.391	0.840	
231557	7.372	3.538	2.970	2.054	0.795	0.427	0.819	
231638	7.387	3.500	2.955	2.053	0.781	0.394	0.841	
231750	7.369	3.544	2.978	2.062	0.801	0.415	0.810	
231839	7.376	3.541	2.962	2.075	0.783	0.412	0.826	
231919	7.385	3.494	2.930	2.057	0.816	0.398	0.838	
232003	7.391	3.531	2.934	2.034	0.783	0.392	0.841	
232051	7.409	3.469	2.913	2.025	0.750	0.371	0.865	
232136	7.382	3.547	2.958	2.049	0.779	0.402	0.833	
232220	7.382	3.547	2.950	2.056	0.781	0.412	0.838	
232700	8.533	3.052	2.543	1.671	0.627	0.276	0.630	comp.

TABLE A3. *Photometric V-band data for II Peg as obtained from the Fine Error Sensor on IUE.*

Date	UT	V	Date	UT	V
14 Aug 1989	22:30	7.64	15 Aug 1989	23:13	7.46
	23:15	7.60	16 Aug 1989	00:41	7.44
15 Aug 1989	00:54	7.61		01:18	7.43
	01:34	7.58		03:14	7.45
	03:10	7.63		06:26	7.35
	06:25	7.50		08:34	7.39
	07:47	7.52		09:21	7.39
	08:26	7.51		09:59	7.42
	09:47	7.49		11:21	7.40
	10:26	7.50		12:01	7.38
	11:50	7.53		13:06	7.42
	12:28	7.57		13:44	7.42
	13:55	7.62		15:09	7.42
	14:44	7.63		15:53	7.39
	16:16	7.58		16:36	7.38
	16:54	7.56		17:38	7.33
	18:16	7.50		18:55	7.37
	18:56	7.49		19:39	7.37
	20:58	7.43		20:56	7.34
	22:33	7.45			

TABLE A4. *Photometric UBVRI data for II Peg as obtained from the Konkoly Observatory. The data are differences with respect to BD +27 4648.*

JD	ΔV	Δ(U-B)	Δ(B-V)	Δ(V-R)	Δ(V-I)
2447754.390	-1.907	-0.141	-0.001	0.106	0.230
2447755.387	-2.043	-0.137	-0.009	0.092	0.206

TABLE A5. *Photometric $UBV(RI)_{KC}$ data for II Peg as obtained from the SAAO. The data are differences with respect to HD 224 084.*

HJD	V	(B-V)	(U-B)	(V-R)	(V-I)
2447727.614	7.42	1.02	0.70	0.60	1.21
2447728.620	7.33	1.02	0.65	0.59	1.21
2447730.616	7.48	1.04	0.60	0.59	1.34
2447741.595	7.38	1.02	0.67	0.60	1.22
2447742.576	7.34	1.02	0.66	0.58	1.21
2447743.574	7.44	1.03	0.66	0.61	1.23
2447744.572	7.54	1.04	0.67	0.60	1.24
2447745.569	7.73	1.07	0.70	0.62	1.30
2447746.558	7.69	1.04	0.73	0.62	1.29
2447748.549	7.37	1.02	0.63	0.59	1.21
2447755.539	7.36	1.03	0.66	0.59	1.22
2447759.527	7.76	1.08	0.75	0.64	1.32
2447760.525	7.63	1.04	0.69	0.62	1.25
2447764.509	7.49	1.04	0.66	0.56	1.22
2447779.479	7.76	1.07	0.73	0.63	1.31
2447792.480	7.69	1.03	0.62	0.60	1.28
2447794.454	7.60	1.05	0.69	0.61	1.27
2447803.392	7.38	1.02	0.68	0.60	1.22
2447805.408	7.57	1.01	0.72	0.59	1.25
2447807.382	7.67	1.03	0.66	0.62	1.27
2447811.388	7.43	1.02	0.52	0.61	1.23
2447838.325	7.42	1.05	0.67	0.59	1.19
2447841.312	7.71	1.05	0.73	0.63	1.30
2447842.309	7.53	1.02	0.71	0.62	1.24
2447843.306	7.38	1.02	0.64	0.57	1.22
2447847.321	7.71	1.06	0.71	0.62	1.29
2447849.302	7.48	1.05	0.68	0.62	1.25
2447850.289	7.37	1.02	0.64	0.59	1.22
2447851.299	7.37	1.03	0.64	0.57	1.20

TABLE A6. *Photometric UBV data for II Peg as obtained from the Stephanion Observatory. The data are differences with respect to BD +27 4648, BD +28 4667 and BD +28 4668.*

JD	V	(B-V)	(U-B)
2447741.5235	7.440	1.031	0.586
2447741.5273	7.435	1.039	0.589
2447741.5353	7.435	1.046	0.596
2447741.5391	7.440	1.046	0.619
2447743.5042	7.468	1.029	0.584
2447743.5092	7.461	1.056	0.591
2447743.5194	7.458	1.033	0.580
2447743.5244	7.428	1.043	0.589
2447744.5155	7.575	1.043	0.569
2447744.5195	7.571	1.056	0.590
2447744.5280	7.570	1.053	0.583
2447744.5310	7.561	1.048	0.590
2447745.5139	7.789	1.061	0.602
2447745.5171	7.789	1.070	0.599
2447745.5247	7.742	1.080	0.632
2447745.5286	7.759	1.071	0.629
2447748.5389	7.436	1.017	0.532
2447750.5370	7.495	1.039	0.551
2447750.5402	7.479	1.035	0.547
2447750.5481	7.466	1.051	0.549
2447750.5516	7.495	1.026	0.539
2447751.4962	7.584	1.029	0.531
2447751.4997	7.585	1.032	0.550
2447751.5085	7.623	1.046	0.558
2447751.5119	7.628	1.035	0.566
2447752.5122	7.784	1.081	0.583
2447752.5155	7.808	1.069	0.603
2447752.5231	7.797	1.075	0.582
2447752.5265	7.787	1.088	0.605

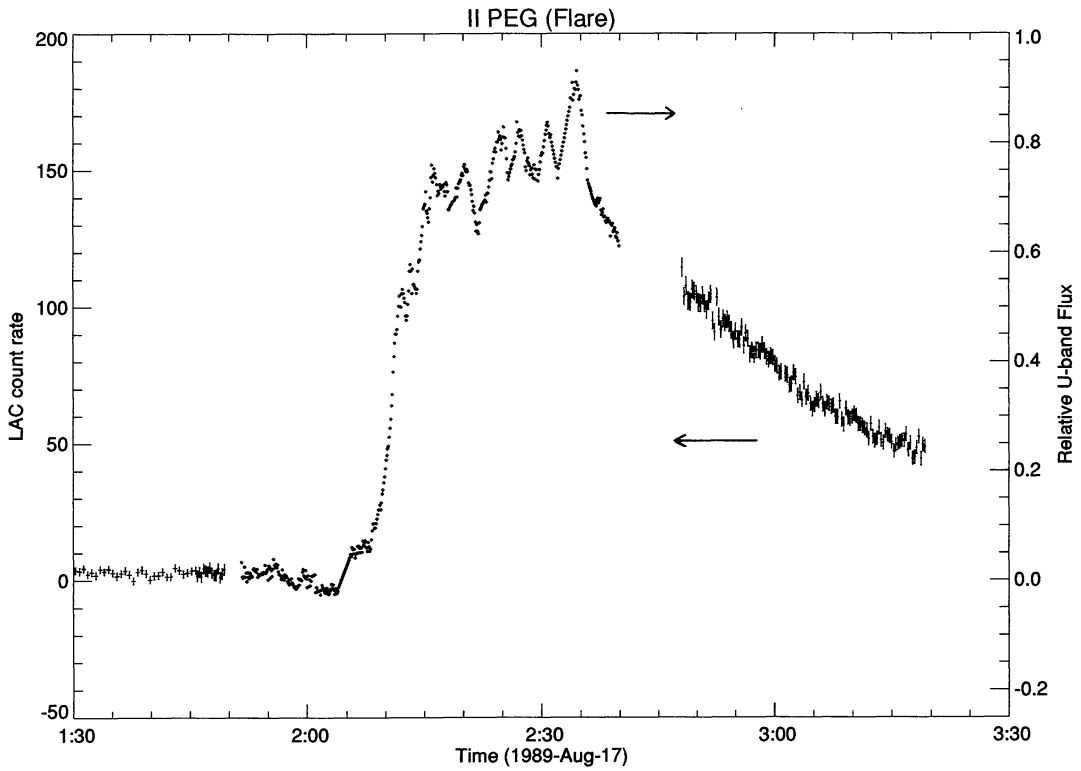

FIGURE 1. A composite Johnson U-band (o) and X-ray (1 – 10 keV) light-curve (†) for the flare detected on II Peg 17 August 1989. Time is given in UT from 17 August 1989

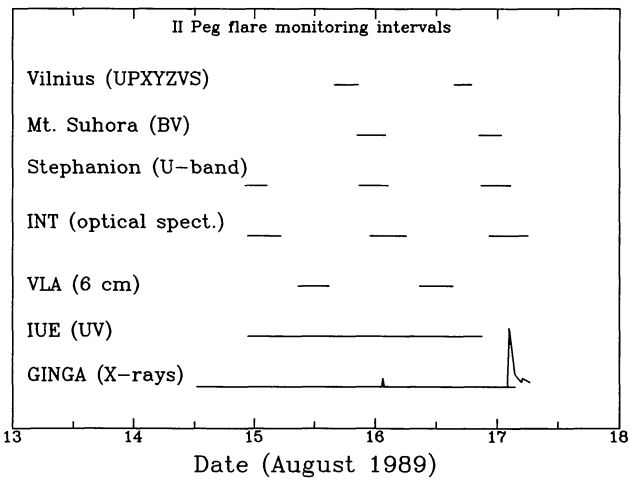

FIGURE 2. The time-lines of the flare monitoring periods for X-ray data from GINGA, the ultraviolet data from IUE, the 3.6, 6 and 20 cm data from the VLA, the red and blue spectroscopy from the INT (La Palma), the U-band data from Stephanion (Greece), the B and V-band data from Mt. Suhora (Poland) and the $UPXYZVS$ data from Mt. Maidanak (Vilnius data). Note that there are small gaps in each of the above time-lines due to observing a standard star, data read-out, computer crash, detectors shut-off, etc. see text for details

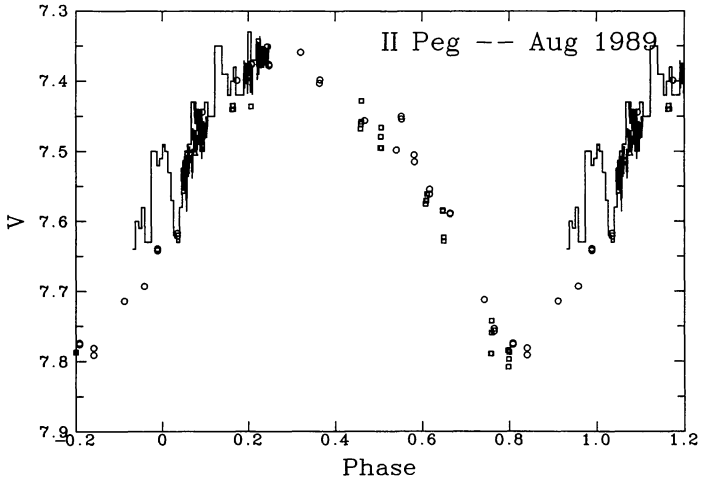

FIGURE 3. V-band photometry for II Peg in August 1989 from SAAO (o), Stephanion (□), Konkoly Observ. (△) and FES (large histogram plot). Data from Mt. Suhora, Vilnius and Athens are the heavy histograms. Note that the SAAO data points at phases 0.99 and 0.035 were taken one and four weeks respectively after the FES and/or Mt. Suhora data

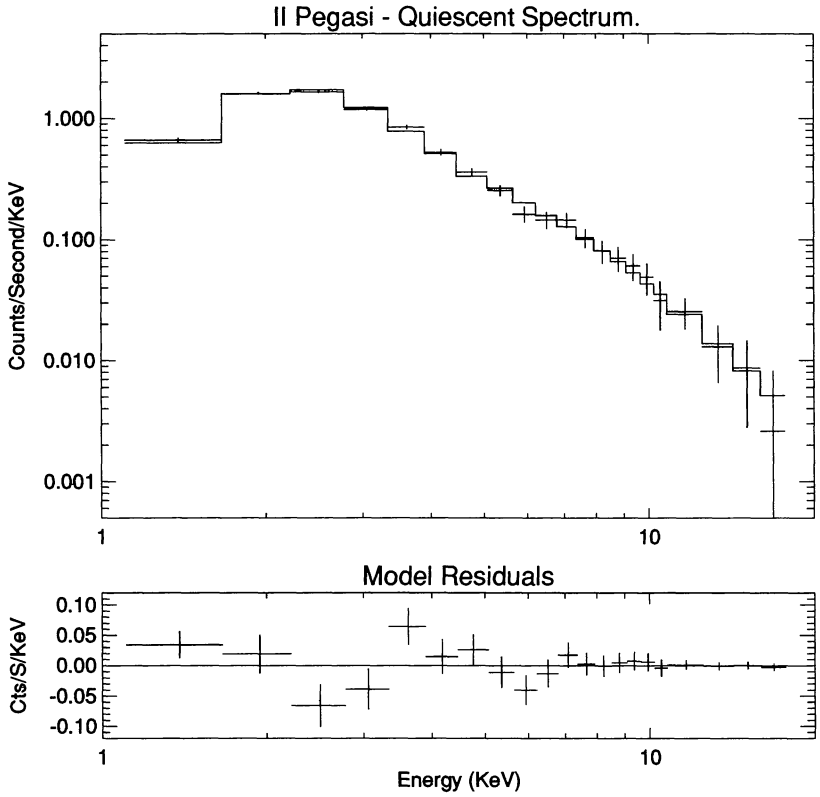

FIGURE 4. The quiescent data for II Peg obtained with GINGA in August 1989 (+), plus a model fit of a single temperature Raymond & Smith model ($T = 12.4 \times 10^6$ K) plus a power-law of $\gamma = 2.05$ for the high energy points. The power-law tail starts becoming prominent at about 6 keV and extends up to 18keV

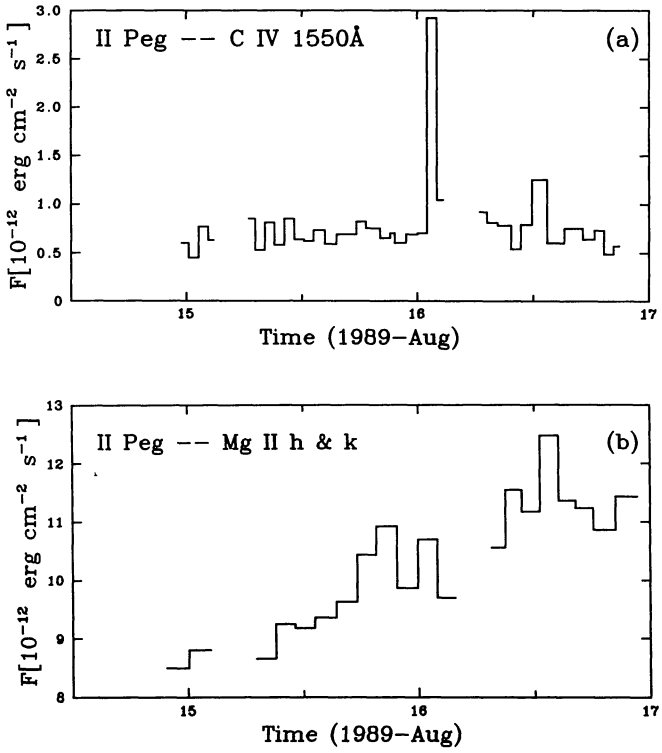

FIGURE 5. Observed fluxes of the C IV 1550Å (a) and Mg II h & k (b) emission lines as observed by IUE from August 15 to August 17, 1989. The time axis is in days

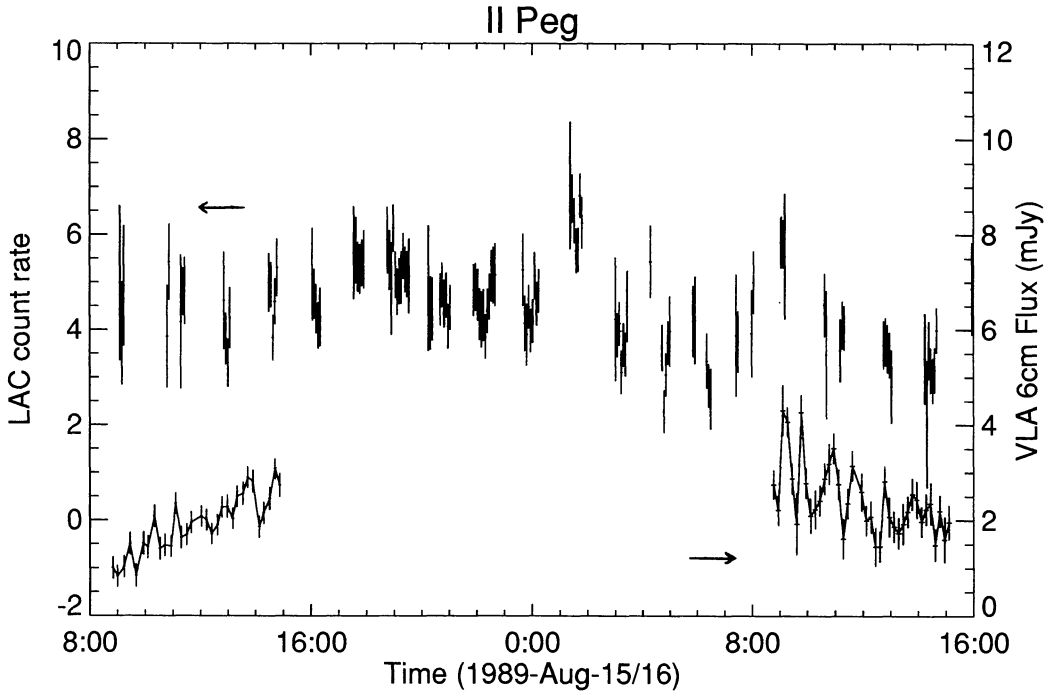

FIGURE 6. A plot of the 6 cm VLA flux in Jy (lower curve) plus the LAC countrate in ct s^{-1} (upper curve) as a function of time from the start of the GINGA observations. The time axis is in hours from 00:00 UT on 14 August 1989

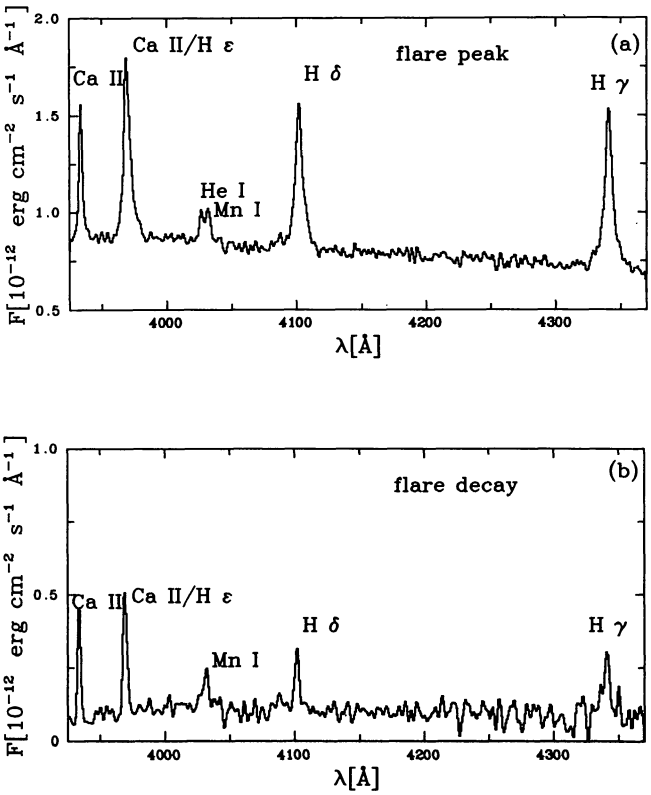

FIGURE 7. (a) The flare-only spectrum (i.e. a mean quiescent spectrum has been subtracted) for II Peg in the blue at around the peak of the 17 August flare (~ 2:18 UT) and (b) a flare only spectrum late in the flare decay phase (~ 4:50 UT)

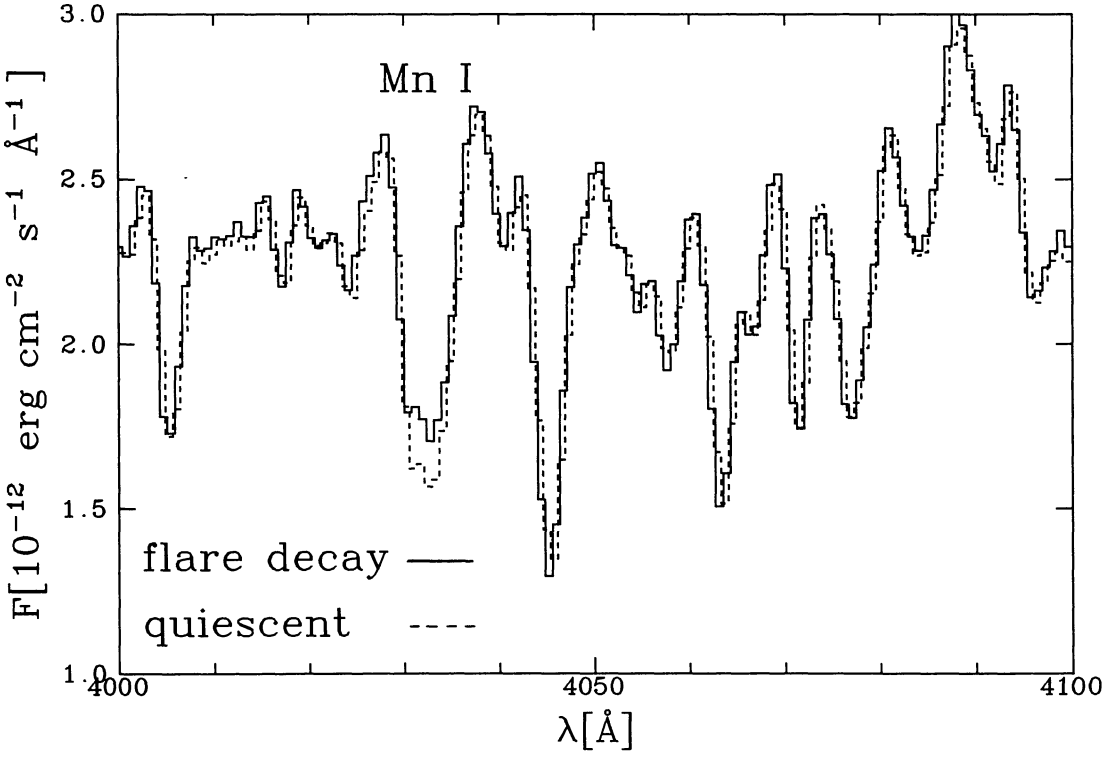

FIGURE 8. The observed spectrum in the region of Mn I 4032Å late in the flare decay (~ 4:50 UT) (– – –) of the observations, plus the mean quiescent spectrum (– – –) superimposed. Note that a small value of 0.1×10^{-12} erg cm^{-2} s^{-1} Å^{-1} has been added to the quiescent spectrum in order to match the depth of absorption features close to Mn I

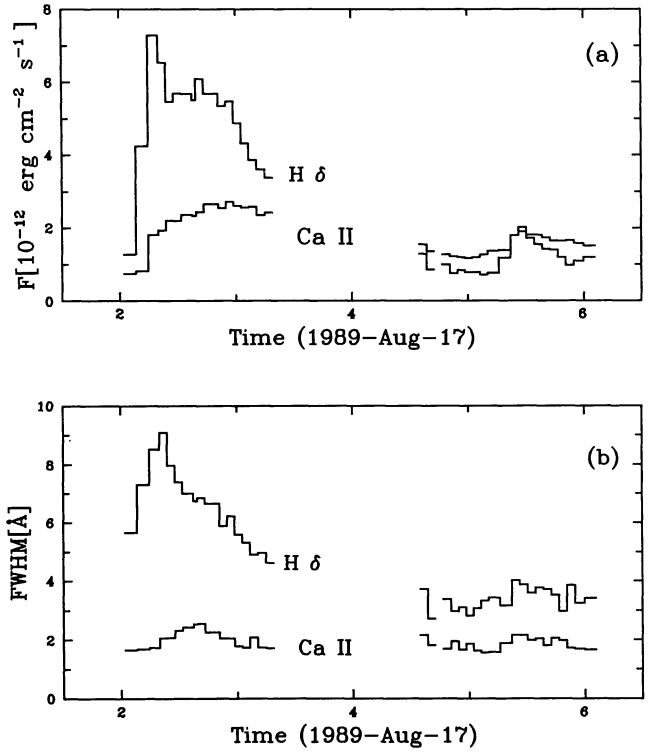

FIGURE 9. **(a)** The line flux in Ca II 3933Å and H δ lines as a function of time from 02:00 UT to 06:00 UT on 17 August 1989 and **(b)** the FWHM of the above two lines during the same interval

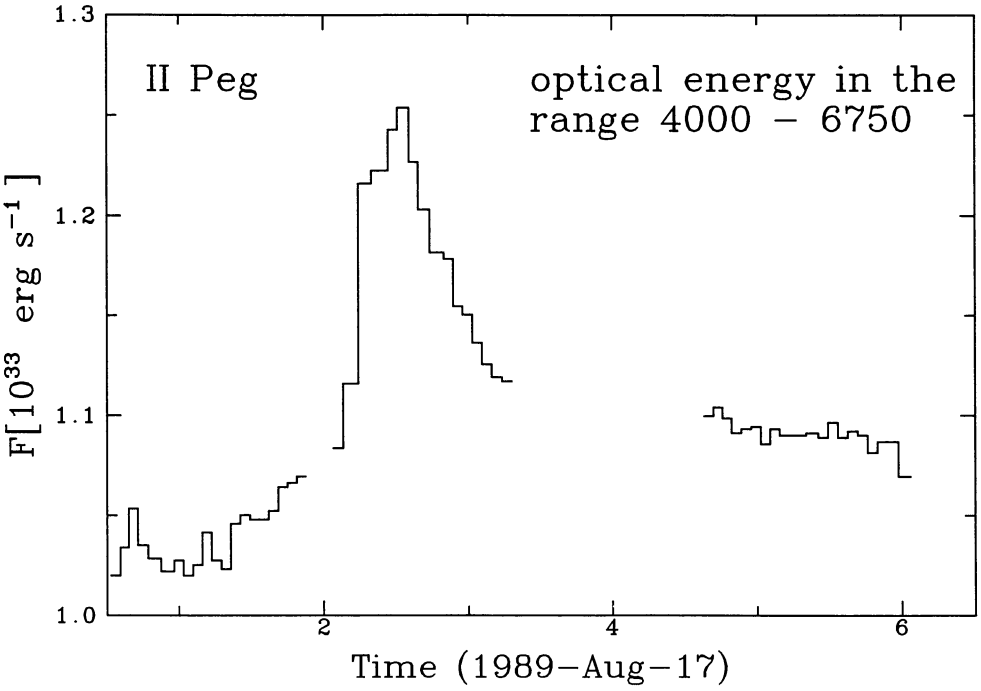

FIGURE 10. The continuum power radiated by II Peg in the range 4000 – 6750Å is shown as a function of time (17 August 1989, 00:30 UT to 06:00 UT). A distance of 29.4 pc to II Peg has been assumed

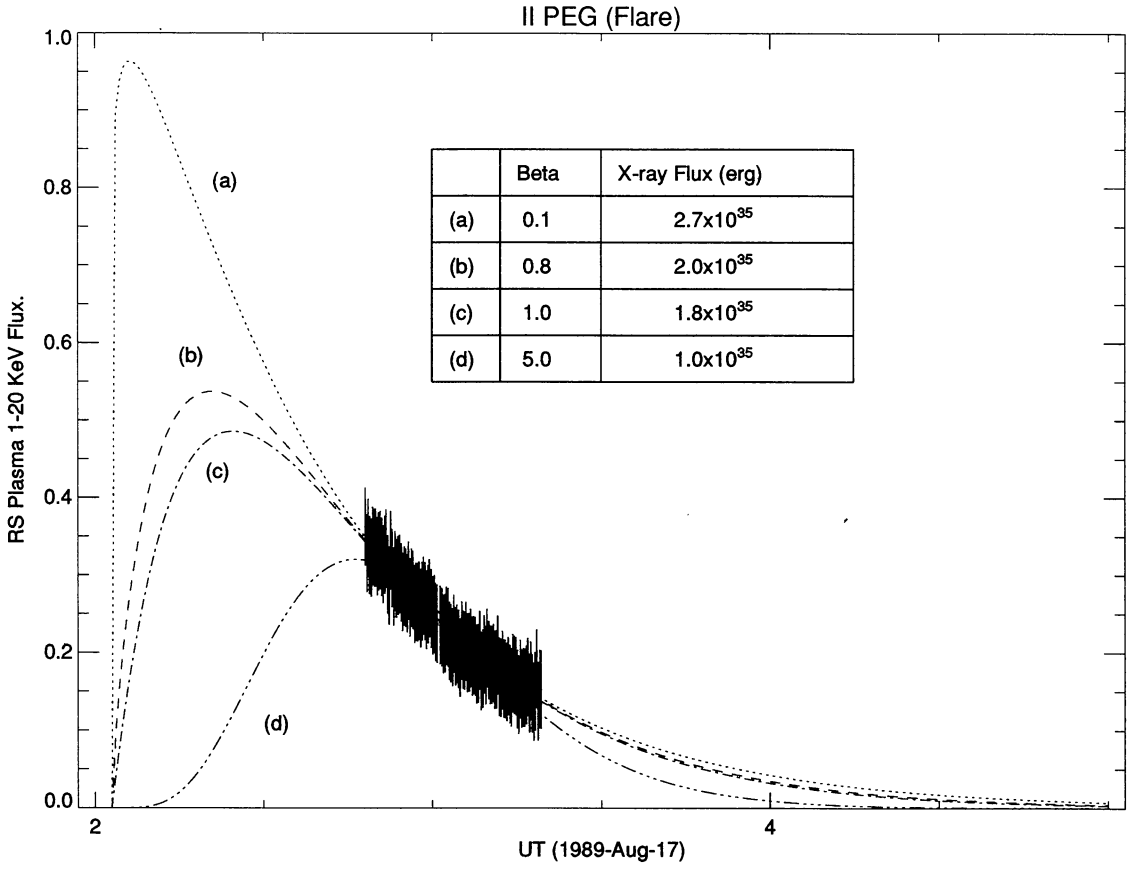

FIGURE 11. Sample "simple burst model" fits to the X-ray data for four values of β: (a) $\beta = 0.1$, (b) $\beta = 0.8$, (c) $\beta = 1.0$ and (c) $\beta = 5.0$. The total integrated X-ray flare energy is given for each model